2002

Rare charm decays in the standard model and beyond

G Burdman

E Golowich
golowich@physics.umass.edu

J Hewett

S Pakvasa

February 1, 2008
LBNL-49074
SLAC-PUB-9057
UH-511-957-01

Rare Charm Decays in the Standard Model and Beyond

Gustavo Burdman[a], Eugene Golowich[b], JoAnne Hewett[c] and Sandip Pakvasa[d]

[a] *Lawrence Berkeley National Laboratory*
Berkeley, CA 94720

[b] *Physics Department, University of Massachusetts,*
Amherst, MA 01003

[c] *Stanford Linear Accelerator Center, Stanford, CA 94309*

[d] *Department of Physics and Astronomy, University of Hawaii,*
Honolulu, HI 96822

Abstract

We perform a comprehensive study of a number of rare charm decays, incorporating the first evaluation of the QCD corrections to the short distance contributions, as well as examining the long range effects. For processes mediated by the $c \to u\ell^+\ell^-$ transitions, we show that sensitivity to short distance physics exists in kinematic regions away from the vector meson resonances that dominate the total rate. In particular, we find that $D \to \pi\ell^+\ell^-$ and $D \to \rho\ell^+\ell^-$ are sensitive to non-universal soft-breaking effects in the Minimal Supersymmetric Standard Model with R-parity conservation. We separately study the sensitivity of these modes to R-parity violating effects and derive new bounds on R-parity violating couplings. We also obtain predictions for these decays within extensions of the Standard Model, including extensions of the Higgs, gauge and fermion sectors, as well as models of dynamical electroweak symmetry breaking.

1 Introduction

The remarkable success of the Standard Model (SM) in describing all experimental information currently available suggests that the quest for deviations from it should be directed either at higher energy scales or at small effects in low energy observables. To the latter group belong the sub-percent level precision measurements of electroweak observables at LEP and SLD as well as the Tevatron experiments [1]. Tests of the SM through quantum corrections have proved to be a powerful tool for probing the high energy scales possibly related to electroweak symmetry breaking and the flavor problem. The absence of flavor changing neutral currents (FCNC) at tree level in the SM implies that processes involving these currents are a primary test of the quantum structure of the theory. Most of the attention on FCNC has been focused on processes involving K and B mesons, such as $K^0 - \bar{K}^0$ and $B^0_{d(s)} - \bar{B}^0_{d(s)}$ mixing and also on rare decays involving transitions such as $s \to d\ell^+\ell-$, $s \to d\nu\bar{\nu}$, $b \to s\gamma$, $b \to s\ell^+\ell^-$, *etc.*

The analogous FCNC processes in the charm sector have received considerably less scrutiny. This is perhaps due to the fact that, on general grounds, the SM expectations are very small both for $D^0 - \bar{D}^0$ mixing [2,3,4] as well as for FCNC decays [5,6,7]. For instance, there are no large non-decoupling effects arising from a heavy fermion in the leading one-loop contributions. This is in sharp contrast with K and B FCNC processes, which are affected by the presence of the top quark in loops. In the SM, D meson FCNC transitions involve the rather light down-quark sector which translates into an efficient GIM cancellation. In many cases, extensions of the SM may upset this suppression and give contributions sometimes orders of magnitude larger than the SM. In this paper we wish to investigate this possibility. As a first step, and in order to establish the existence of a clean window for the observation of new physics in a given observable in rare charm processes, we must compute the SM contribution to such quantities. This is of particular importance in this case due to the presence of potentially large long-distance contributions which are non-perturbative in essence and therefore non-calculable by analytical methods. In general the flavor structure of charm FCNC favors the propagation of light-quark-states as intermediate states which, if dominant, obscure the more interesting short distance contributions that are the true test of the SM. This is the situation in $D^0 - \bar{D}^0$ mixing [2,3,4] and in the $c \to u\gamma$ transition [5]. In the case of mixing, although the long distance effects seem to dominate over the SM short distance contributions, it is still possible that there is a window of one or two orders of magnitude between these and the current experimental limit [8]; the predictions of numerous extensions of the SM lie in this window [9]. On the other hand, charm radiative decays are completely dominated by non-perturbative physics and do not constitute a suitable test of the short distance structure of the SM or its extensions.

In what follows we investigate the potential of rare charm decays to constrain exten-

sions of the SM. With the exception of $D^0 \to \gamma\gamma$, we shall concentrate on the non-radiative FCNC transitions such as $c \to u\ell^+\ell^-$, $c \to u\nu\bar{\nu}$ which enter in decays like $D^0 \to \mu^+\mu^-$, $D \to X_u\ell^+\ell^-$, $D \to X_u\nu\bar{\nu}$, *etc.* We extensively consider supersymmetry by studying the Minimal Supersymmetric SM (MSSM) as well as supersymmetric scenarios allowing R-parity violation. We find that rare charm decays are potentially good tests of the MSSM and also serve to constrain R-parity violating couplings in kinematic regions away from resonances. In charged dilepton modes, this mostly means at *low* dilepton mass. In general, we find that this kinematic region, corresponding to large hadronic recoil, is the most sensitive for new physics searches.

The $D \to V\ell^+\ell^-$ decays were studied in Ref. [10] in the SM without QCD corrections. More recently the $D \to \pi\ell^+\ell^-$ decays were examined in Ref. [11] in the SM and some of its extensions, including the MSSM. We compare these predictions with ours, and find some discrepancies in the SM calculation of the long distance contributions. We also emphasize the importance of $D \to V\ell^+\ell^-$ in the MSSM due to its enhanced sensitivity to the electromagnetic dipole moment operator entering in $c \to u\gamma$.

In the next section we calculate the SM short distance contributions including QCD corrections and estimate long distance effects for various decay modes. In Section 3 we study possible extensions of the SM that might produce signals which fall below current experimental limits but above the SM results of Section 2. We summarize and conclude in Section 4.

As a final comment, we note the following convention and notation used throughout the paper. Many quantities relating to both SM and also new physics are chiral, involving projection operators for left-handed (LH) and right-handed (RH) massless fermions. We shall employ the notation

$$\Gamma_{\rm L,R} \equiv \frac{1 \pm \gamma_5}{2} \ , \qquad \Gamma^\mu_{\rm L,R} \equiv \frac{\gamma^\mu(1 \pm \gamma_5)}{2} \tag{1}$$

for scalar projection operators $\Gamma_{\rm L,R}$ and vector projection operators $\Gamma^\mu_{\rm L,R}$. The chiral projections of fermion field q are thus expressed as

$$q_{\rm L,R} \ \equiv \ \Gamma_{\rm L,R}\ q \ \ . \tag{2}$$

2 The Standard Model Contributions

In this section we study the Standard Model contributions to various charm meson rare decays. At the time of this writing, there are no reported events of the type we are considering. We group the decay modes by their common short distance structure. In each case we address both the perturbative short distance amplitude and the effects of the non-perturbative long-range propagation of intermediate hadronic states. Due to

the non-perturbative nature of the underlying physics, the long distance effects cannot be calculated with controlled uncertainties. Therefore we find it prudent to generate estimates by using several distinct approaches, such as vector meson dominance (VMD) for processes with photon emission and/or calculable unitarity contributions. In this way, we hope to obtain a reasonable measure of the uncertainty involved in the calculation, and at the same time, obtain bounds on the magnitude of long-distance contributions which are not overly model dependent.

2.1 Meson Lepton-antilepton Transitions $D \to X\ell^+\ell^-$

As we shall discuss, this mode is likely to be observed at forthcoming B and Charm factory/accelerator experiments. We start with the calculation of both short and long distance contributions to the inclusive rate. We then compute the rates for various exclusive modes.

2.1.1 The Short Distance Contribution to $D \to X_u\ell^+\ell^-$

The short distance contribution is induced at one loop in the SM. It is convenient to use an effective description with the W boson and the b-quark being integrated out as their thresholds are reached, respectively, in the renormalization group evolution [12],

$$\begin{aligned}
\mathcal{H}_{\rm eff} &= -\frac{4G_F}{\sqrt{2}}\left[\sum_{q=d,s,b} C_1^{(q)}(\mu)O_1^{(q)}(\mu) + C_2^{(q)}(\mu)O_2^{(q)}(\mu) + \sum_{i=3}^{10} C_i(\mu)O_i(\mu)\right]\ ,\ m_b < \mu < M_W \\
\mathcal{H}_{\rm eff} &= -\frac{4G_F}{\sqrt{2}}\left[\sum_{q=d,s} C_1^{(q)}(\mu)O_1^{(q)}(\mu) + C_2^{(q)}(\mu)O_2^{(q)}(\mu) + \sum_{i=3}^{10} C'_i(\mu)O'_i(\mu)\right]\ ,\ \mu < m_b\,, \qquad (3)
\end{aligned}$$

with $\{O_i\}$ being the complete operator basis, $\{C_i\}$ the corresponding Wilson coefficients and μ the renormalization scale; the primed quantities indicate those where the b-quark has been eliminated. Note that we must keep all terms of order $1/M_W^2$ above the scale $\mu = m_b$ in this decay as opposed to radiative decays. In Eq. (3), the Wilson coefficients contain the dependence on the Cabibbo-Kobayashi-Maskawa (CKM) matrix elements $V_{qq'}$. As was pointed out in Ref. [5], the CKM structure of these transitions is drastically different from that of the analogous B meson processes. The operators O_1 and O_2 are explicitly split into their CKM components

$$O_1^{(q)} = (\bar{u}_L^\alpha \gamma_\mu q_L^\beta)(\bar{q}_L^\beta \gamma^\mu c_L^\alpha)\ , \qquad O_2^{(q)} = (\bar{u}_L^\alpha \gamma_\mu q_L^\alpha)(\bar{q}_L^\beta \gamma^\mu c_L^\beta)\ , \qquad (4)$$

where $q = d, s, b$, and α, β are contracted color indices. The rest of the operator basis is defined in the standard way. The QCD penguin operators are given by

$$O_3 = (\bar{u}_L^\alpha \gamma_\mu c_L^\alpha)\sum_q (\bar{q}_L^\beta \gamma^\mu q_L^\beta)\ , \qquad O_4 = (\bar{u}_L^\alpha \gamma_\mu c_L^\beta)\sum_q (\bar{q}_L^\beta \gamma^\mu q_L^\alpha)\ ,$$

$$O_5 \;=\; (\bar{u}_L^\alpha \gamma_\mu c_L^\alpha) \sum_q (\bar{q}_R^\beta \gamma^\mu q_R^\beta) \;, \qquad O_6 = (\bar{u}_L^\alpha \gamma_\mu c_L^\beta) \sum_q (\bar{q}_R^\beta \gamma^\mu q_R^\alpha) \quad , \tag{5}$$

the electromagnetic and chromomagnetic dipole operators are

$$O_7 = \frac{e}{16\pi^2} m_c (\bar{u}_L \sigma_{\mu\nu} c_R) F^{\mu\nu} \;, \qquad O_8 = \frac{g_s}{16\pi^2} m_c (\bar{u}_L \sigma_{\mu\nu} T^a c_R) G_a^{\mu\nu} \quad , \tag{6}$$

and finally the four-fermion operators coupling directly to the charged leptons are

$$O_9 = \frac{e^2}{16\pi^2} (\bar{u}_L \gamma_\mu c_L)(\bar{\ell}\gamma^\mu \ell) \;, \qquad O_{10} = \frac{e^2}{16\pi^2} (\bar{u}_L \gamma_\mu c_L)(\bar{\ell}\gamma^\mu \gamma_5 \ell) \quad . \tag{7}$$

The matching conditions at $\mu = M_W$ for the Wilson coefficients of the operators O_{1-6} are

$$C_1^q(M_W) = 0 \;, \qquad C_{3-6}(M_W) = 0 \;, \qquad C_2^q(M_W) = -\lambda_q \quad , \tag{8}$$

with $\lambda_q = V_{cq}^* V_{uq}$. The corresponding conditions for the coefficients of the operators O_{7-10} are

$$\begin{aligned}
C_7(M_W) &= -\frac{1}{2}\left\{\lambda_s F_2(x_s) + \lambda_b F_2(x_b)\right\} \quad , \\
C_8(M_W) &= -\frac{1}{2}\left\{\lambda_s D(x_s) + \lambda_b D(x_b)\right\} \quad , \\
C_9^{(\prime)}(M_W) &= \sum_{i=s,(b)} \lambda_i \left[-\Big(F_1(x_i) + 2\bar{C}(x_i)\Big) + \frac{\bar{C}(x_i)}{2s_w^2} \right] \quad , \\
C_{10}^{(\prime)}(M_W) &= -\sum_{i=s,(b)} \lambda_i \frac{\bar{C}(x_i)}{2s_w^2} \quad .
\end{aligned} \tag{9}$$

In Eqs. (9) we define $x_i = m_i^2/M_W^2$, the functions $F_1(x)$, $F_2(x)$ and $\bar{C}(x)$ are those derived in Ref. [13] and the function $D(x)$ was defined in Ref. [5].

To compute the $c \to u\ell^+\ell^-$ rate at leading order, operators in addition to O_7, O_9 and O_{10} must contribute. Even in the absence of the strong interactions, the insertion of the operators $O_2^{(q)}$ in a loop would give a contribution sometimes referred to as leading order mixing of C_2 with C_9. When the strong interactions are included, further mixing of the four-quark operators with O_{7-10} occurs. The effect of these QCD corrections in the renormalization group (RG) running from M_W down to $\mu = m_c$ is of particular importance in $C_7^{\rm eff}(m_c)$, the coefficient determining the $c \to u\gamma$ amplitude. As was shown in Ref. [5], the QCD-induced mixing with $O_2^{(q)}$ dominates $C_7^{\rm eff}(m_c)$. The fact that the main contribution to the $c \to u\gamma$ amplitude comes from the insertion of four-quark operators inducing light-quark loops signals the presence of large long distance effects. This was confirmed in Ref. [5] where these non-perturbative contributions were estimated and found to dominate the rate. Therefore, in the present calculation we will take into account effects of the strong interactions in $C_7^{\rm eff}(m_c)$. On the other hand, as mentioned above, the

operator O_9 mixes with four-quark operators even in the absence of QCD corrections [14]. Finally, the RG running does not affect O_{10}, *i.e.* $C_{10}(m_c) = C_{10}(M_W)$. Thus, in order to estimate the $c \to u\ell^+\ell^-$ amplitude it is a good approximation to consider the QCD effects only where they are dominant, *i.e.* in $C_7^{\rm eff}(m_c)$, whereas we expect these to be less dramatic in $C_9^{\rm eff}(m_c)$.

The leading order mixing of $O_2^{(q)}$ with O_9 results in

$$C_9^{(\prime)\ {\rm eff}} = C_9^{(\prime)}(M_W) + \sum_{i=d,s,(b)} \lambda_i \left[-\frac{2}{9}\,\ln\frac{m_i^2}{M_W^2} + \frac{8}{9}\frac{z_i^2}{\hat{s}} - \frac{1}{9}\left(2 + \frac{4z_i^2}{\hat{s}}\right)\sqrt{\left|1 - \frac{4z_i^2}{\hat{s}}\right|}\ \mathcal{T}(z_i)\right] , \tag{10}$$

where we have defined

$$\mathcal{T}(z) = \begin{cases} 2\ \arctan\left[\frac{1}{\sqrt{\frac{4z^2}{\hat{s}}-1}}\right] & (\text{for } \hat{s} < 4z^2) \\ \\ \ln\left|\frac{1+\sqrt{1-\frac{4z^2}{\hat{s}}}}{1-\sqrt{1-\frac{4z^2}{\hat{s}}}}\right| - i\pi & (\text{for } \hat{s} > 4z^2)\ , \end{cases} \tag{11}$$

and $\hat{s} \equiv s/m_c^2$, $z_i \equiv m_i/m_c$. The logarithmic dependence on the internal quark mass m_i in the second term of Eq. (10) cancels against a similar term in the Inami-Lim function $F_1(x_i)$ entering in $C_9(M_W)$, leaving no spurious divergences in the $m_i \to 0$ limit.

To compute the differential decay rate in terms of the Wilson coefficients, we use the two-loop QCD corrected value of $C_7^{\rm eff}(m_c)$ as obtained in Ref. [6], compute $C_9^{\rm eff}(m_c)$ from Eq. (10), and $C_{10}(m_c) = C_{10}(M_W)$ from Eq. (9). The differential decay rate in the approximation of massless leptons is given by

$$\begin{aligned} \frac{d\Gamma_{c\to u\ell^+\ell^-}}{d\hat{s}} &= \tau_D\ \frac{G_F^2\alpha^2 m_c^6}{768\pi^5}\ (1-\hat{s})^2 \left[\left(\left|C_9^{(\prime)\ {\rm eff}}(m_c)\right|^2 + |C_{10}|^2\right)(1+2\hat{s})\right. \\ &\left. +12\ C_7^{\rm eff}(m_c)\ {\rm Re}\left[C_9^{(\prime)\ {\rm eff}}(m_c)\right] + 4\left(1+\frac{2}{\hat{s}}\right)\left|C_7^{\rm eff}(m_c)\right|^2\right] , \end{aligned} \tag{12}$$

where τ_D refers to the lifetime of either $D^\pm$ or D^0. We estimate the inclusive branching ratios for $m_c = 1.5$ GeV, $m_s = 0.15$ GeV, $m_b = 4.8$ GeV and $m_d = 0$,

$$\mathcal{B}r^{\rm (sd)}_{D^+\to X_u^+ e^+e^-} \simeq 2\times 10^{-8}\ , \qquad \mathcal{B}r^{\rm (sd)}_{D^0\to X_u^0 e^+e^-} \simeq 8\times 10^{-9}\ . \tag{13}$$

It is useful to observe that the dominant contributions to the rates in Eq. (13) come from the leading order mixing of O_9 with the four-quark operators $O_2^{(q)}$, the second term in Eq. (10). As noted above, the dominance of light-quark intermediate states in the short distance contributions is a signal of the presence of large long distance effects. However, when considering the contributions of various new physics scenarios, it should be kept in

Table 1: Examples of $D \to PV^0 \to P\ell^+\ell^-$ Mechanism.

Mode	$\mathcal{B}r^{(\mathrm{pole})}$	$\mathcal{B}r^{(\mathrm{expt})}$
$D^+ \to \pi^+\phi \to \pi^+e^+e^-$	$1.8 \cdot 10^{-6}$	$< 5.2 \cdot 10^{-5}$
$D^+ \to \pi^+\phi \to \pi^+\mu^+\mu^-$	$1.5 \cdot 10^{-6}$	$< 1.5 \cdot 10^{-5}$
$D_s^+ \to \pi^+\phi \to \pi^+e^+e^-$	$1.1 \cdot 10^{-5}$	$< 2.7 \cdot 10^{-4}$
$D_s^+ \to \pi^+\phi \to \pi^+\mu^+\mu^-$	$0.9 \cdot 10^{-5}$	$< 1.4 \cdot 10^{-4}$

mind that their magnitudes must be compared to the mixing of these operators. Shifts in the matching conditions for the Wilson coefficients C_7, C_9 and C_{10}, even when large, are not enough to overwhelm the long distance effects in most extensions of the SM. These considerations will be helpful when we evaluate what type of new physics scenarios might be relevant in these decay modes.

2.1.2 The Long Distance Contributions to $D \to X_u\ell^+\ell^-$

As a first estimate of the contributions of long distance physics we will consider the resonance process $D \to XV \to X\ell^+\ell^-$, where $V = \phi, \rho, \omega$. We isolate contributions from this particular mechanism by integrating $d\Gamma/dq^2$ over each resonance peak associated with an exchanged vector or pseudoscalar meson. The branching ratios thus obtained (we refer to each such branching ratio as $\mathcal{B}r^{(\mathrm{pole})}$) are in the $\mathcal{O}(10^{-6})$ range. Modes experiencing the largest effects are displayed in Table 1 (see also Ref. [15]), where we compare our theoretically derived branching ratios with existing experimental bounds [16]. Due to the small $\eta \to \ell^+\ell^-$ and $\eta' \to \ell^+\ell^-$ branching ratios, the dominant contributions arise from V^0 exchange.

This result suggests that the long distance contributions overwhelm the short distance physics and possibly any new physics that might be present. However, as we will see below this is not always the case. A more thorough treatment requires looking at all the kinematically available regions in $D \to X_u\ell^+\ell^-$, not just the resonance region. In order to do this, the effect of these states can be thought of as a shift in the short distance coefficient C_9^{eff} in Eq. (10), since $V \to \ell^+\ell^-$ selects a vector coupling for the leptons. This follows from Ref. [17], which incorporates in a similar manner the resonant contributions to $b \to q\ell^+\ell^-$ decays via a dispersion relation for $\ell^+\ell^- \to$ hadrons. This procedure is manifestly gauge invariant. The new contribution can be written via the replacement [17]

$$C_9^{\mathrm{eff}} \to C_9^{\mathrm{eff}} + \frac{3\pi}{\alpha^2} \sum_i \kappa_i \frac{m_{V_i}\Gamma_{V_i \to \ell^+\ell^-}}{m_{V_i}^2 - s - i m_{V_i}\Gamma_{V_i}} \ , \tag{14}$$

where the sum is over the various relevant resonances, m_{V_i} and Γ_{V_i} are the resonance mass and width, and the factor $\kappa_i \sim \mathcal{O}(1)$ is a free parameter adjusted to fit the non-leptonic decays $D \to XV_i$ when the V_i are on shell. We obtain $\kappa_\phi \simeq 3.6$, $\kappa_\rho \simeq 0.7$ and $\kappa_\omega \simeq 3.1$. The last value comes from assuming $\mathcal{B}r_{D^+\to\pi^+\omega} = 10^{-3}$, since a direct measurement is not available yet.

As a first example we study the $D^+ \to \pi^+ e^+ e^-$ decay. The main long-distance contributions come from the ϕ, ρ and ω resonances. The η and η' effects are negligibly small. The dilepton mass distribution for this decay takes the form

$$\frac{d\Gamma}{ds} = \frac{G_F^2\alpha^2}{192\pi^5}|\mathbf{p}_\pi|^3\,|f_+(s)|^2\,\left(\left|\frac{2m_c}{m_D}C_7^{\rm eff} + C_9^{\rm eff}\right|^2 + |C_{10}|^2\right)\,, \tag{15}$$

where $s = m_{ee}^2$ is the squared of the dilepton mass. Here we have make use of the heavy quark spin symmetry relations that relate the matrix elements of O_7 to the "semileptonic" matrix elements of O_9 and O_{10} [18]. An additional form-factor is formally still present, but its contribution to the decay rate is suppressed by $(m_\ell/m_D)^2$ and is neglected here. For the form-factor $f_+(s)$ we make use of the prediction of Chiral Perturbation Theory for Heavy Hadrons [19], which at low recoil gives

$$f_+(s) = \frac{f_D}{f_\pi}\frac{g_{D^*D\pi}}{(1 - s/M_{D^*}^2)}\,, \tag{16}$$

where we use the recent CLEO measurement [20] $g_{D^*D\pi} = 0.59 \pm 0.1 \pm 0.07$, and we take $f_D = 200$ MeV. In Fig. 1 we present this distribution as a function of the dilepton mass. The two narrow peaks are the ϕ and the ω, which sit on top of the broader ρ. The total rate results in $\mathcal{B}r_{D^+\to\pi^+e^+e^-} \simeq 2\times 10^{-6}$. Although most of this branching ratio arises from the intermediate $\pi^+\phi$ state, we can see from Figure 1 that new physics effects as low as 10^{-7} can be observed as long as such sensitivity is achieved in the regions away from the ω and ϕ resonances, both at low and high dilepton mass squared.

Similarly, we can consider the decay $D^+ \to \rho^+ e^+ e^-$. Since there is less data available at the moment on the $D \to VV'$ modes, we will take the values of the κ_i in Eq. (14) from the fits to the $D^+ \to \pi^+ V$ case studied above. For the semileptonic form-factors we use the extracted values from the $D \to K^*\ell\nu$ data [21] and assuming $SU(3)$ symmetry[1]. The total integrated branching ratio is $\mathcal{B}r_{D^0\to\rho^0 e^+e^-} = 1.8\times10^{-6}$ (*i.e.* $\mathcal{B}r_{D^+\to\rho^+e^+e^-} = 4.5\times10^{-6}$). As can be seen in Fig. 2, once again most of this rate comes from the resonance contributions. However, there is also a region -in this case confined to low values of m_{ee} due to the kinematics- where sensitive measurements could test the SM short distance structure of these transitions. In addition, the ρ modes contain angular information in the form of a forward-backward asymmetry for the lepton pair. Since this asymmetry arises as

[1]The $D \to \rho$ form-factors will be extracted with precision at Charm and B factories. In the meantime, we do not believe the assumption of $SU(3)$ symmetry will affect our main conclusions here.

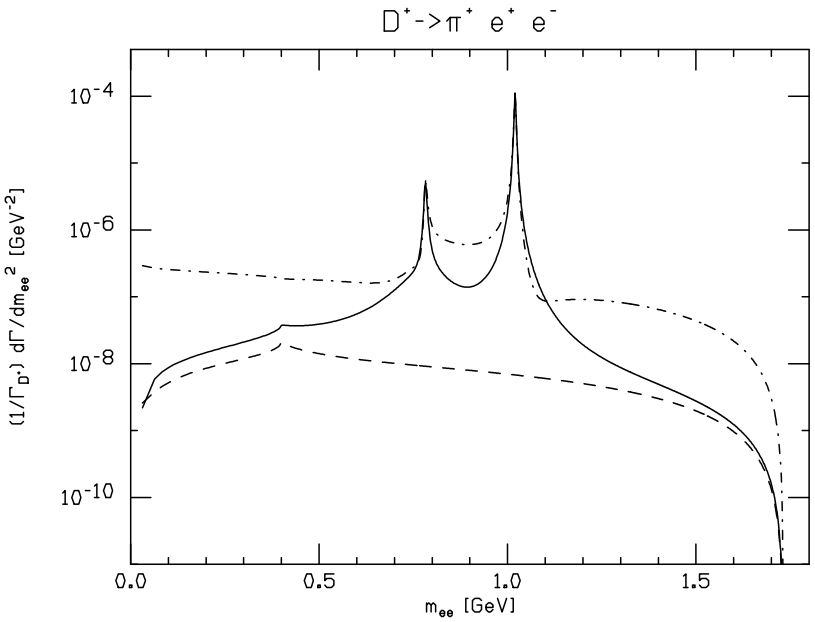

Figure 1: The dilepton mass distribution for $D^+ \to \pi^+ e^+ e^-$, normalized to Γ_{D^+}. The solid line shows the sum of the short and the long distance SM contributions. The dashed line corresponds to the short distance contribution only. The dot-dash line includes the allowed R-parity violating contribution from Supersymmetry (see Section 3.1.2)

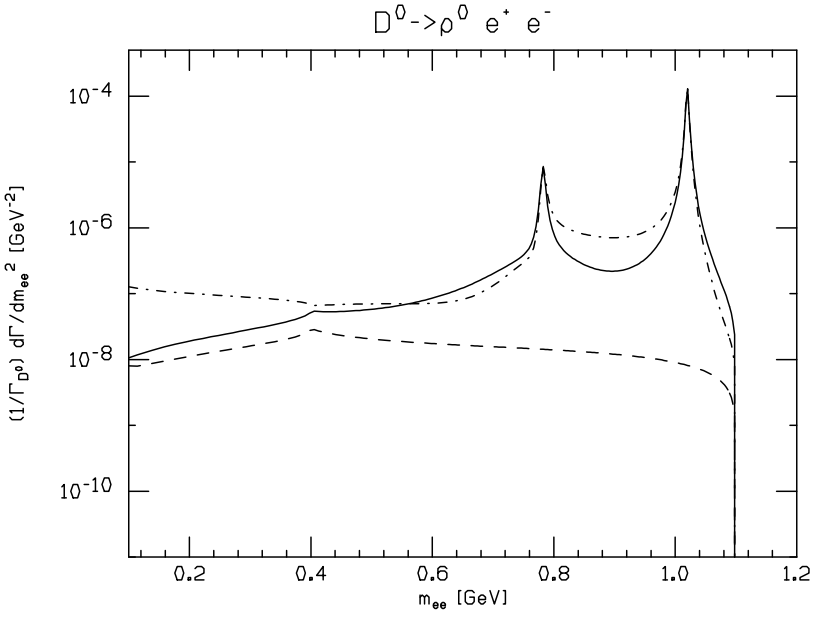

Figure 2: The dilepton mass distribution for $D^0 \to \rho^0 e^+ e^-$, normalized to Γ_{D^0}. The solid line shows the sum of the short and the long distance SM contributions. The dashed line corresponds to the short distance contribution only. The dot-dash line includes the allowed R-parity violating contribution from Supersymmetry (see Section 3.1.2)

a consequence of the interference between the vector and the axial-vector couplings of the leptons, it is negligible in the SM since the vector couplings due to vector mesons overwhelm the axial-vector couplings. This is true even away from the resonance region, partly because of the large width of the ρ and partly since the coefficient $C_9^{(\prime)\text{eff}}$ and $C_7^{(\prime)\text{eff}}$ get large enhancements due to mixing with O_2 and from the QCD corrections, whereas C_{10} -the axial-vector coupling- is not affected by any of these. This results in a very small interference. We expand on this point and consider the possibility of large asymmetries from physics beyond the SM in Section 3.1.2. For both the π and ρ modes the sensitivity to new physics effects is reserved to large $\mathcal{O}(1)$ enhancements since the long distance contributions are still important even when away from the resonances.

We finally compare our results in Figs. 1 and 2 with those obtained in Refs. [10] and [11]. The short distance calculations in both these papers do not include the tree-level mixing of O_9 with O_2. This effect determines most of the short distance amplitude. Also, as mentioned above, this piece cancels the logarithm in Eq. (10), a scheme dependent term of no physical significance. If this cancellation did not take place the logarithm would be the largest contribution to C_9. In addition, in Ref [10] the QCD corrections are not included. We also differ in the long distance results, which dominate these decays. For $D \to \pi\ell^+\ell^-$ the authors of Ref. [10] make use of the factorization approximation, as well as heavy hadron chiral perturbation theory for both pseudoscalars and vector mesons. It is far from clear that the use of both approximations in D decays is warranted. For the case of $D \to \rho\ell^+\ell^-$, the results of Ref. [11] show a large enhancement at low q^2 when compared with Fig. 2. However, a $1/q^2$ enhancement can only appear as a result of non-factorizable contributions. This is clear from Ref. [22] and [23]: the factorization amplitude for $D \to \rho V$, when combined with a gauge invariant $(\gamma - V)$ mixing, leads to a null contribution to $D \to V\ell^+\ell^-$. This is due to the fact that the mixing of the operator O_2 with O_7 is non-factorizable [23]. A resonant contribution to O_7, leading to a $1/q^2$ behavior, is then proportional to C_7^{eff}, which is mostly given by the O_2 mixing. In addition, when compared with the usual short distance matrix element of O_7, this resonant contribution will be further suppressed by the factor $g_V(q^2)A^{\text{nf}}(q^2)$, where $g_V(q^2)$ is the $(\gamma - V)$ mixing form-factor, and $A^{\text{nf}}(q^2)$ parametrizes the non-factorizable amplitude $\langle\rho V|O_7|D\rangle$, which is of $\mathcal{O}(\Lambda_{\text{QCD}}/m_c)$ [24]. Thus, even if we take the on-shell values for these quantities, the resonant contribution to O_7 is likely to be below 10% of the SM short distance contribution. The actual off-shell values at low q^2 far from the resonances are likely to be even smaller. We then conclude that the $1/q^2$ enhancement is mostly given by the short distance contribution. This is only noticeable at extremely small values of the dilepton mass, so that it is likely to be beyond the experimental sensitivity in the electron modes (due to Dalitz conversion), whereas in the muon modes it lies beyond the physical region. On the other hand, the factorizable pieces contribute to the matrix elements of O_9, just as in Eq. (14), and give no enhancement at low values of q^2.

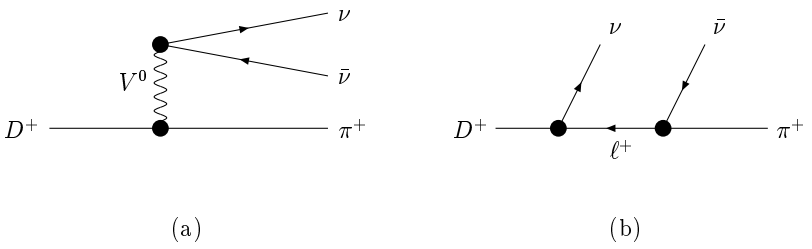

(a) (b)

Figure 3: Some long distance contributions.

2.2 Neutrino-antineutrino Emission $D \to P\nu_\ell\bar{\nu}_\ell$

In the Standard Model, decays such as

$$D^+(p) \to \pi^+(p')\ \nu_\ell(k)\ \bar{\nu}_\ell(\bar{k}) \qquad \text{and} \qquad D^0(p) \to \bar{K}^0(p')\ \nu_\ell(k)\ \bar{\nu}_\ell(\bar{k}) \tag{17}$$

will have branching ratios which are generally (but, as we shall show, not always) too small to measure. Such decays thus represent attractive modes for new physics searches.

2.2.1 The Short Distance Contribution $c \to u\nu_\ell\bar{\nu}_\ell$

These decay modes are induced by Z penguin as well as box diagrams. The corresponding effective hamiltonian takes the form

$$\mathcal{H}_{\rm eff} = \frac{G_F}{\sqrt{2}}\frac{\alpha}{2\pi s_W^2}\sum_{\ell=e,\mu,\tau}\Big\{\lambda_s X^\ell(x_s) + \lambda_b X^\ell(x_b)\Big\}\,(\bar{u}_L\gamma_\mu c_L)(\bar{\nu}_L^\ell\gamma^\mu\nu_L^\ell)\ . \tag{18}$$

The functions in Eq. (18) are defined by $X^\ell(x_i) = \bar{D}(x_i, m_\ell)/2$, with the functions $\bar{D}$ given in Ref. [13]. Although we have explicitly kept the dependence on the charged lepton masses arising from the box diagrams, this is of numerical significance only when considering the strange quark contributions with an internal tau lepton. In any case, the branching ratios in the SM are unobservably small. For instance, one has

$$\mathcal{B}r^{(\rm s.d.)}_{D^+\to X_u\nu\bar{\nu}} \simeq 1.2\times 10^{-15}\ , \qquad \mathcal{B}r^{(\rm s.d.)}_{D^0\to X_u\nu\bar{\nu}} \simeq 5.0\times 10^{-16}\ \ , \tag{19}$$

where the contributions of all neutrinos have been included.

2.2.2 Long Distance Contributions to $D \to P\nu_\ell\bar{\nu}_\ell$

Long-distance contributions to the exclusive transition $D \to P\nu_\ell\bar{\nu}_\ell$ (P is a pseudoscalar meson) can have just hadrons, just leptons or both hadrons and leptons in the intermediate state. Examples of the first two cases are depicted respectively in Fig. 3(a) and Fig. 3(b).

As a simple model of the purely hadronic intermediate state, we consider in detail the non-leptonic weak process $D(p) \to \pi(p')V^0(q)$ followed by the conversion $V^0(q) \to$

$\nu_\ell(k)\bar{\nu}_\ell(\bar{k})$, *cf* Fig. 3(a). We determine first the $V^0 \to \nu_\ell\bar{\nu}_\ell$ ($V^0 = \phi, \rho^0, \omega$) vertex, which has the invariant amplitude

$$\mathcal{M}_{V^0\to\nu_\ell\bar{\nu}_\ell} \simeq \left(\frac{g_2}{2\cos\theta_w}\right)^2 \frac{1}{M_Z^2}\ \bar{u}(k)\Gamma_\mu^{\rm L} v(\bar{k})\ \langle 0|\ \sum_q J_q^\mu\ |V^0\rangle \quad , \tag{20}$$

where J_q^μ is the current coupling quark q to the Z gauge boson. Only the vector part of the current contributes and we find

$$\mathcal{M}_{V^0\to\nu_\ell\bar{\nu}_\ell} \simeq \frac{2G_F}{\sqrt{2}} h_V \bar{u}(k)\epsilon_V^\mu \Gamma_\mu^{\rm L} v(\bar{k}) \quad . \tag{21}$$

Using the measured electromagnetic transitions $V^0 \to \ell^+\ell^-$ ($V^0 = \rho^0, \omega, \phi$) as input, we find for the coupling h_V

$$|h_V| = \begin{cases} (3/2 - 2s_w^2)M_\phi^2/f_\phi \simeq 0.112\ \text{GeV}^2 & (V=\phi) \\ (9/8 - 2s_w^2)M_\rho^2/f_\rho - 3M_\omega^2/8f_\omega \simeq 0.107\ \text{GeV}^2 & (V=\rho) \\ -(9/8 - 2s_w^2)M_\omega^2/f_\omega + 3M_\rho^2/8f_\rho \simeq 0.008\ \text{GeV}^2 & (V=\omega) \end{cases} , \tag{22}$$

where we adopt the numerical values of f_ϕ, f_ρ, f_ω listed in Ref. [22].

The corresponding transition amplitude for the non-leptonic D decay process is then

$$\mathcal{M}^{(\rm V^0)}_{D\to P\nu_\ell\bar{\nu}_\ell} = G_F^2 M_D^2 \frac{1}{q^2 - (M_V - i\Gamma_V/2)^2} F(q^2) h_V(q^2) \bar{u}(k) p'\cdot\gamma\Gamma_{\rm L} v(\bar{k}) \quad , \tag{23}$$

where $q \equiv p - p' = k + \bar{k}$ is the four-momentum carried by the virtual vector meson and $F(q^2)$ appears in the $D \to V^0 P$ amplitude. We find for the q^2-distribution

$$\frac{d\Gamma_{D\to P\nu_\ell\bar{\nu}_\ell}}{dq^2} = \frac{G_F^4 M_D^4}{192\pi^3}\frac{|\mathbf{p}'|}{M_D^2}\frac{F^2(q^2)h_V^2(q^2)}{(q^2 - M_V^2)^2 + \Gamma_V^2 M_V^2}\left((q\cdot p')^2 - \frac{q^2 M_V^2}{4}\right) . \tag{24}$$

We have used data from non-leptonic decays into pseudoscalar-vector final states ($D \to P + V^0$) to serve as input for $D^+ \to \pi^+\nu_\ell\bar{\nu}_\ell$ (ρ^0 pole), $D^0 \to \bar{K}^0\nu_\ell\bar{\nu}_\ell$ (ρ^0, ω, ϕ poles) and $D_s^+ \to \pi^+\nu_\ell\bar{\nu}_\ell$ (ω, ϕ poles). Taking the largest contributor in each category, we obtain

$$\begin{aligned} \mathcal{B}r_{D^+\to\pi^+\nu\bar{\nu}} &\simeq 5.1\times 10^{-16} \qquad (V=\rho^0) \\ \mathcal{B}r_{D^0\to\bar{K}^0\nu\bar{\nu}} &\simeq 2.4\times 10^{-13} \qquad (V=\phi) \\ \mathcal{B}r_{D_s^+\to\pi^+\nu\bar{\nu}} &\simeq 7.8\times 10^{-15} \qquad (V=\phi) \quad , \end{aligned} \tag{25}$$

where we have summed over the three neutrino flavors. Although this analysis pertains to just the amplitudes of Fig. 3(a), we believe our results reflect the order of magnitude to be expected for other hadronic intermediate states as well. All such processes lead to unmeasurably small branching ratios.

There will also be amplitudes with single lepton intermediate states, as in Fig. 3(b). For electron and muon intermediate states, the amplitude for $D(p) \to P(p')\nu_\ell(k)\bar{\nu}_\ell(\bar{k})$ is reducible to

$$\mathcal{M}^{(\text{lept.})}_{D\to P\nu_{(e,\mu)}\bar{\nu}_{(e,\mu)}} = -2G_F^2 V_{ud}V_{cd}^*\bar{u}(k)p\cdot\gamma\Gamma_{\rm L}v(\bar{k}) + \mathcal{O}(m^2_{(e,\mu)}) \quad . \tag{26}$$

These lead to the branching ratios

$$\mathcal{B}r_{D^+\to\pi^+\nu_{(e,\mu)}\bar{\nu}_{(e,\mu)}} \simeq 1.8\times 10^{-16} \ , \qquad \mathcal{B}r_{D_s^+\to\pi^+\nu_{(e,\mu)}\bar{\nu}_{(e,\mu)}} \simeq 3.8\times 10^{-15} \quad , \tag{27}$$

which are again too small for detection.

There remains the case in which τ^+ propagates as the intermediate state. This differs from the above cases involving e and μ propagation in that for part of the ν_τ-$\bar{\nu}_\tau$ phase space, the intermediate τ^+ is on the mass shell. The mode $D_s^+ \to \tau^+ + \nu_\tau$ has been observed[2] with $\mathcal{B}r_{D_s^+\to\tau^+\nu_\tau} = (7\pm 4)\%$ whereas $D^+ \to \tau^+ + \nu_\tau$ has not (the predicted branching ratio is $\mathcal{B}r_{D^+\to\tau^+\nu_\tau} \simeq 9.2\ 10^{-4}$). Once the on-shell τ^+ has been produced, its branching ratio to decay into a given meson can be appreciable, *e.g.* $\mathcal{B}r_{\tau\to\rho^+\bar{\nu}_\tau} \simeq 0.25$, $\mathcal{B}r_{\tau\to\pi^+\bar{\nu}_\tau} \simeq 0.11$, *etc.* Such transitions, although involving production of a $\nu\bar{\nu}$ pair in the final state, should be measurable at a B and/or Charm factory.

2.3 Two Photon Emission $D^0 \to \gamma\gamma$

The amplitude for the transition $D^0(p) \to \gamma(q_1,\lambda_1)\gamma(q_2,\lambda_2)$ can be expressed as

$$\mathcal{M}_{D^0\gamma\gamma} = \epsilon_\mu^\dagger(1)\epsilon_\nu^\dagger(2)\left[(q_1^\nu q_2^\mu - q_1\cdot q_2\ g^{\mu\nu})\ C_{D^0\gamma\gamma} + i\epsilon^{\mu\nu\alpha\beta}q_{1\alpha}q_{2\beta}\ B_{D^0\gamma\gamma}\right] \quad . \tag{28}$$

The invariant amplitudes $B_{D^0\gamma\gamma}$ and $C_{D^0\gamma\gamma}$ are P-conserving and P-violating, respectively, and carry units of inverse energy. They contribute to the $D^0 \to \gamma\gamma$ branching ratio as

$$\mathcal{B}r_{D^0\to\gamma\gamma} = \frac{M_D^3\tau_{D^0}}{64\pi}\left[\ |B_{D^0\gamma\gamma}|^2 + |C_{D^0\gamma\gamma}|^2\ \right] \quad . \tag{29}$$

The amplitude in Eq. (28) is sometimes written in the equivalent form

$$\mathcal{M}_{D^0\gamma\gamma} = \frac{C_{D^0\gamma\gamma}}{2}F_1^{\mu\nu}F_{2\mu\nu} + i\frac{B_{D^0\gamma\gamma}}{2}F_{1\mu\nu}\tilde{F}_{2\mu\nu} \quad , \tag{30}$$

where $F^{\mu\nu} \equiv i(q^\mu\epsilon^\nu - q^\nu\epsilon^\mu)$ and $\tilde{F}^{\mu\nu} \equiv \epsilon^{\mu\nu\alpha\beta}F_{\alpha\beta}/2$.

[2]In this experiment, only the leptonic decay mode $\tau^+ \to \ell\nu_\ell\bar{\nu}_\tau$ was detected. [25]

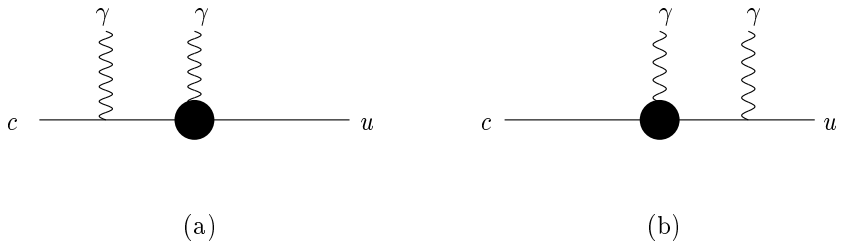

Figure 4: $1PR$ contributions to $c \to u\gamma\gamma$.

2.3.1 The Short Distance Contribution $c\bar{u} \to \gamma\gamma$

Consider the quark level transition $c \to u\gamma\gamma$. This can arise via one-particle irreducible (1PI) processes in which both photons arise from the interaction vertex or one-particle reducible (1PR) processes in which at least one of the photons is radiated from the initial state c-quark or final state u-quark.

To estimate the $c \to u\gamma\gamma$ amplitude, we employ an approximation which makes use of known results on the related process $c \to u\gamma$. According to Ref. [6], the two-loop $c \to u\gamma$ vertex is

$$\mathcal{M}^{(\mathrm{s.d.})}_{cu\gamma} = \frac{4G_F}{\sqrt{2}} \frac{e}{16\pi^2} A m_c \sigma_{\mu\nu} \Gamma_{\mathrm{R}} F^{\mu\nu} \quad , \tag{31}$$

where $|A| \simeq 0.0047$. Keeping in mind that there are additional diagrams which must be accounted for in a complete two-loop analysis, we shall use this as input to the 1PR graphs depicted in Fig. 4. The dominant contribution to the $c \to u\gamma\gamma$ amplitude involves photon emission from the u-quark. To ensure that the effect is indeed 'short-range', we follow the locality procedure employed in Ref. [26]. This yields for $c\bar{u} \to \gamma\gamma$ the amplitude

$$|B^{(\mathrm{s.d.})}_{D^0\gamma\gamma}| = |C^{(\mathrm{s.d.})}_{D^0\gamma\gamma}| = \frac{G_F \alpha}{3\sqrt{2}\pi} \frac{m_c}{M_D - m_c} \; f_D \; |A| \quad , \tag{32}$$

resulting in the branching ratio

$$\mathcal{B}r^{(\mathrm{s.d.})}_{D^0 \to \gamma\gamma} \; \simeq \; 3 \times 10^{-11} \quad , \tag{33}$$

for the choice $M_D - m_c \simeq 0.3$ GeV.

2.3.2 Long Distance Contributions to $D^0 \to \gamma\gamma$

We shall model long-distance contributions to the $D^0 \to \gamma\gamma$ amplitude using the vector meson dominance (VMD) mechanism and the unitarity constraint. The latter can only be done in a limited context since there will be many unitarity contributions. We will consider several one-particle intermediate states (as used in $K \to \gamma\gamma$ decays) as well as the two-particle K^+K^- intermediate state.

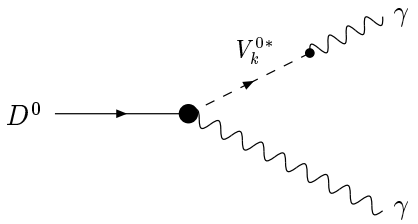

Figure 5: Vector dominance (VMD) contribution.

Vector Meson Dominance

One can view (*c.f.* Fig. 5) the $D^0 \to \gamma\gamma$ amplitude as the single VMD process

$$D^0 \to \gamma \ + \ \sum_k \ V_k^{0*} \ \to \ \gamma + \gamma \ \ . \tag{34}$$

We have previously used the VMD mechanism to model the general single-photon emission $D \to M + \gamma$ (M is some non-charm meson) [5]. It is straightforward to extend our analysis to the $D^0 \to \gamma\gamma$ mode, as long as care is taken in the $D^0 \to \gamma\gamma$ amplitude to ensure gauge invariance and Bose-Einstein statistics. The amplitudes used in the $D^0(p) \to V^0(k) + \gamma(q)$ transition are defined as

$$\mathcal{M}_{DV\gamma} = \epsilon_V^{\mu\dagger}(k,\lambda_V)\epsilon_\gamma^{\nu\dagger}(q,\lambda_\gamma)\left[C_V(k_\nu q_\mu - k\cdot q g_{\mu\nu}) + iB_V\epsilon_{\mu\nu\alpha\beta}k^\alpha q^\beta\right] \ \ . \tag{35}$$

The VMD amplitude that we calculate is therefore of the form

$$B_{D^0\gamma\gamma}^{(\mathrm{vmd})} = \sum_i \ \frac{2e}{f_{V_i}} \ B_{V_i} \ \eta_i \ , \qquad C_{D^0\gamma\gamma}^{(\mathrm{vmd})} = \sum_i \ \frac{2e}{f_{V_i}} \ C_{V_i} \ \eta_i \ \ , \tag{36}$$

where f_V is the coupling for the $V^0 - \gamma$ conversion amplitude, the index 'i' refers to the specific vector meson (ρ^0, ω^0, ϕ^0) and η_i is a factor accounting for the VMD extrapolation made in q^2. We take $\eta_i \simeq 1/2$ as a reasonable choice.

The values in Table 2 are somewhat lower than those which would be obtained from the $V\gamma$ amplitudes in Ref. [5]. The main reason for this is the central value for $\mathcal{B}r_{D^0\to\phi\rho^0}$, which is a numerically significant input to the VMD calculation, cited in the Particle Data Group compilation has decreased by a factor of about three between 1994 and 2000. Using the central values in Table 2 and assuming positive interference between the various amplitudes to provide the maximal VMD signal gives the branching ratio

$$\mathcal{B}r_{D^0\to\gamma\gamma}^{(\mathrm{vmd})} = \left(3.5\ {}^{+4.0}_{-2.6}\right) \times 10^{-8} \ \ . \tag{37}$$

Table 2: VMD Amplitudes (10^{-8} GeV^{-1}).

$D^0 \to V^0\gamma$	$B^{\rm vmd}_{D^0\gamma\gamma}$	$C^{\rm vmd}_{D^0\gamma\gamma}$
$D^0 \to \rho^0\gamma$	$0.036\ (1 \pm 0.7)$	$0.045\ (1 \pm 0.3)$
$D^0 \to \omega^0\gamma$	$0.011\ (1 \pm 0.5)$	$0.012\ (1 \pm 0.5)$
$D^0 \to \phi^0\gamma$	$0.047\ (1 \pm 0.7)$	$0.036\ (1 \pm 0.4)$

Single-particle Unitarity Contribution

In this category of amplitudes (*cf.* Fig. 6) the D^0 mixes with a spinless meson (either a pseudoscalar P_n or a scalar S_n) and finally decays into a photon pair,

$$\begin{aligned} B^{(\rm mix)}_{D^0\gamma\gamma} &= \sum_{P_n} \langle P_n|\mathcal{H}^{(\rm p.c.)}_{wk}|D^0\rangle\ \frac{1}{M_D^2 - M_{P_n^2}}\ B_{P_n\gamma\gamma} \\ C^{(\rm mix)}_{D^0\gamma\gamma} &= \sum_{S_n} \langle S_n|\mathcal{H}^{(\rm p.v.)}_{wk}|D^0\rangle\ \frac{1}{M_D^2 - M_{S_n^2}}\ C_{S_n\gamma\gamma}\ \ . \end{aligned} \tag{38}$$

Let us consider two distinct kinds of contributions, $B^{\rm mix}_{D^0\gamma\gamma} = B^{(\rm gnd)}_{D^0\gamma\gamma} + B^{(\rm res)}_{D^0\gamma\gamma}$:

1. If the spinless meson is a ground-state particle (π^0, η or η'),[3] we have

$$B^{\rm gnd}_{D^0\gamma\gamma} = -\frac{G_F a_2 f_D \alpha}{\sqrt{2}\pi}\left[\frac{\xi_d}{\sqrt{2}}\frac{M_\pi^2}{M_D^2 - M_\pi^2} + \frac{2\xi_s - \xi_d}{3\sqrt{2}}\sum_{k=\eta,\eta'}\frac{M_k^2}{M_D^2 - M_k^2} f_k(\theta)\right]\ \ , \tag{39}$$

where $a_2 \simeq -0.55$, $\theta \simeq -20^o$, $f_\eta(\theta) \equiv \cos^2\theta - 2\sqrt{2}\sin\theta\cos\theta$ and $f_{\eta'}(\theta) \equiv \sin^2\theta + 2\sqrt{2}\sin\theta\cos\theta$. The above parameterization for the two-photon vertices agrees with the values determined experimentally,

$$B_{P_n\gamma\gamma} = \left\{\begin{array}{ll} 0.0249\ \text{GeV}^{-1} & (\pi^0) \\ 0.0275\ \text{GeV}^{-1} & (\eta) \\ 0.0334\ \text{GeV}^{-1} & (\eta')\ \ . \end{array}\right. \tag{40}$$

$B^{\rm gnd}_{D^0\gamma\gamma}$ is seen to vanish, as it must, in the limit of SU(3) flavor symmetry (there $\langle\eta'|\mathcal{H}^{(\rm p.c.)}_{wk}|D^0\rangle = 0$ and the π^0, η contributions cancel). From Eq. (29), we obtain the branching ratio

$$\mathcal{B}r^{\rm gnd}_{D^0\to\gamma\gamma}\ \simeq\ 3\times 10^{-11}\ \ . \tag{41}$$

[3]The kaon intermediate state is disfavored due to the small $K \to \gamma\gamma$ branching ratio.

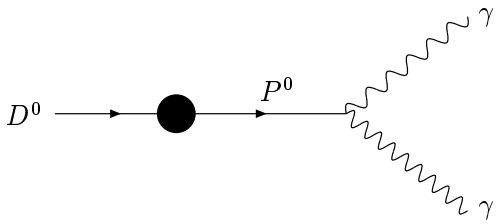

Figure 6: Weak mixing contribution.

2. If the intermediate meson is a spinless resonance R^0, the decay chain becomes $D^0 \to R^0 \to \gamma\gamma$. Since little is yet known about meson excitations, both the weak mixing amplitudes and the two-photon emission amplitudes must be modeled theoretically. The D^0-to-resonance weak matrix element will depend upon the flavor structure of R^0, *e.g.*

$$\langle R^0|\mathcal{H}_{wk}^{(\mathrm{p.c.})}|D^0\rangle = -\frac{G_F a_2 f_D}{\sqrt{2}} \begin{cases} \xi_d f_R/\sqrt{2} & (R^0 = (\bar{u}u - \bar{d}d)/\sqrt{2}) \\ \xi_s f_R & (R^0 = \bar{s}s) \\ V_{cd}^* V_{us} f_R & (R^0 = \bar{s}d)) \end{cases} , \tag{42}$$

where the flavor content of R^0 is in parentheses and estimates for resonance decay constants f_R are given in Ref. [3]. The $R^0 \to \gamma\gamma$ mode has been observed for a number of resonances and has typical branching ratios $\mathcal{B}r_{R^0\to\gamma\gamma} = \mathcal{O}(10^{-5})$ for $M_R \simeq 1 \to 1.3$ GeV, decreasing to $\mathcal{B}r_{R^0\to\gamma\gamma} = \mathcal{O}(10^{-6})$ for $M_R \geq 1.5$ GeV.

For a concrete example of the resonance mechanism, we choose $R^0 = \pi(1800)$ and assume $\mathcal{B}r_{\pi(1800)\to\gamma\gamma} \simeq 10^{-6}$. The resulting $D^0 \to \gamma\gamma$ branching ratio is

$$\mathcal{B}r_{D^0\to\gamma\gamma}^{R^0=\pi(1800)} \sim 10^{-10} . \tag{43}$$

Two-particle Unitarity Contribution

In a factorization approach, the $D^0 \to K^+K^-$ amplitude (*cf.* Fig. 7) is

$$\mathcal{M}_{D^0K^+K^-} = \frac{G_F M_D^2}{\sqrt{2}} V_{cs}V_{us}^* f \left[\left(1 - \frac{M_K^2}{M_D^2}\right) f_+(M_K^2) + \frac{M_K^2}{M_D^2} f_-(M_K^2)\right] , \tag{44}$$

where $f_\pm$ are form factors and f is a constant containing information about QCD corrections and the kaon decay constant. A fit to the measured $D^0 \to K^+K^-$ decay rate yields

$$f\left[\left(1 - \frac{M_K^2}{M_D^2}\right) f_+(M_K^2) + \frac{M_K^2}{M_D^2} f_-(M_K^2)\right] = 141 \text{ MeV} . \tag{45}$$

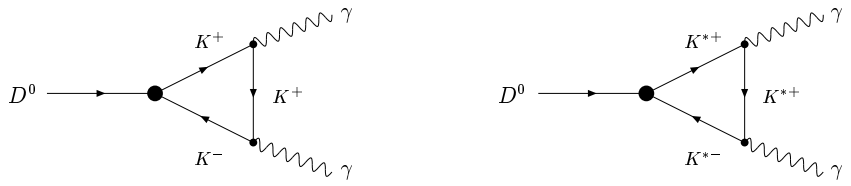

(a) (b)

Figure 7: Unitarity contributions: (a) K^+K^-, (b) $K^{*+}K^{*-}$.

Similar to the B_s system[27], the K^+K^- intermediate state contributes via unitarity to only the amplitude $C_{D^0\gamma\gamma}$ of Eq. (28) and is proportional to precisely the same combination of form factors appearing in Eq. (45),

$$\mathcal{I}m\ C_{D^0\gamma\gamma}^{(K^+K^-)} = 2\alpha \frac{M_K^2}{M_D^4} \sqrt{1 - 4M_K^2/M_D^2}\ \mathcal{M}_{D^0K^+K^-} \quad , \tag{46}$$

from which we obtain

$$\mathcal{B}r_{D^0\to\gamma\gamma}^{(K^+K^-)} \sim 0.7 \times 10^{-8} \quad . \tag{47}$$

Summary of $D^0 \to \gamma\gamma$

Considered together, the above examples lead us to anticipate a branching ratio in the neighborhood of 10^{-8}. Our maximal (*i.e.* constructive interference) VMD signal has a central value $\mathcal{B}r_{D^0\to\gamma\gamma}^{(\rm vmd)} \simeq 3.5 \times 10^{-8}$. The recent work of Ref. [28] provides an independent estimate of the $D^0 \to \gamma\gamma$ transition and obtains a similar order-of-magnitude result.

2.4 Lepton-antilepton Emission $D^0 \to \ell^+\ell^-$

The general form for the amplitude describing $D^0(p) \to \ell^+(k_+, s_+)\ell^-(k_-, s_-)$ is

$$\mathcal{M}_{D^0\to\ell^+\ell^-} = \bar{u}(k_-, s_-)\,[A_{D^0\ell^+\ell^-} \ + \ \gamma_5\ B_{D^0\ell^+\ell^-}]\,v(k_+, s_+) \quad , \tag{48}$$

and the associated decay rate is

$$\Gamma_{D^0\to\ell^+\ell^-} = \frac{M_D}{8\pi}\sqrt{1 - 4\frac{m_\ell^2}{M_D^2}}\left[|A_{D^0\ell^+\ell^-}|^2 \ + \ \left(1 - 4\frac{m_\ell^2}{M_D^2}\right)|B_{D^0\ell^+\ell^-}|^2\right] \quad . \tag{49}$$

2.4.1 Short Distance Contributions $c\bar{u} \to \ell^+\ell^-$

The short distance ($\mathcal{O}(\alpha_s)$ corrected) transition amplitude is given by [14]

$$B_{D^0\ell^+\ell^-}^{(\rm s.d.)} \simeq \frac{G_F^2 M_W^2 f_D m_\ell}{\pi^2} F\,, \tag{50}$$

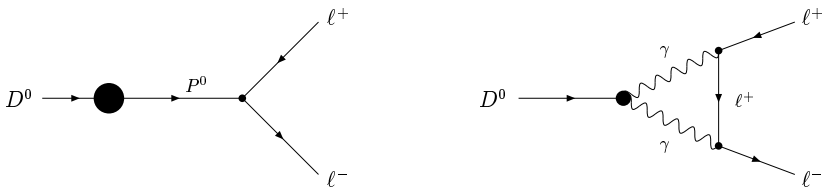

Figure 8: Unitarity contributions: (a) One-particle, (b) Two-particle $\gamma\gamma$.

where

$$F = \sum_{i=d,s,b} V_{ui} V_{ci}^* \left[\frac{x_i}{2} + \frac{\alpha_s}{4\pi} x_i \cdot \left(\ln^2 x_i + \frac{4+\pi^2}{3} \right) \right] , \tag{51}$$

with $x_i = m_i^2/M_W^2$. The amplitude $A_{D^0\ell^+\ell^-}$ vanishes due to the equations of motion. The explicit dependence on lepton mass in the decay amplitude overwhelmingly favors the $\mu^+\mu^-$ final state over that of e^+e^-. Upon employing the quark mass values $m_d \simeq 0.01$ GeV, $m_s \simeq 0.12$ GeV, $m_b \simeq 5.1$ GeV, the Wolfenstein CKM parameters $\lambda \simeq 0.22$, $A \simeq 0.82$, $\rho \simeq 0.21$, $\eta \simeq 0.35$ and the decay constant $f_D \simeq 0.2$ GeV, we obtain the branching fraction $\mathcal{B}r^{s.d.}_{D^0\to\mu^+\mu^-} \simeq 10^{-18}$.

2.4.2 Long Distance Contributions to $D^0 \to \ell^+\ell^-$

In the following, we consider two long distance unitarity contributions (*cf.* Fig. 8) which lead to $D^0 \to \ell^+\ell^-$ transitions. In each case, the decay amplitude is dependent on the lepton mass, and thus we shall provide numerical branching ratios only for the case $D^0 \to \mu^+\mu^-$.

Single-particle Unitarity Contribution

The single-particle 'weak-mixing' contribution to $D^0 \to \ell^+\ell^-$ can be estimated in a manner like that considered for the $D^0 \to \gamma\gamma$ transition (*cf.* Eq. (38)). For definiteness, we consider the $D^0 \to \ell^+\ell^-$ parity-conserving amplitude $B_{D^0\ell^+\ell^-}$ (see Eq. (48)),

$$B^{(\rm mix)}_{D^0\ell^+\ell^-} \;=\; \sum_{P_n} \langle P_n | \mathcal{H}^{(\rm p.c.)}_{wk} | D^0 \rangle \; \frac{1}{M_D^2 - M_{P_n^2}} \; B_{P_n\ell^+\ell^-} \quad , \tag{52}$$

and we write $B^{(\rm mix)}_{D^0\ell^+\ell^-} = B^{(\rm gnd)}_{D^0\ell^+\ell^-} \; + \; B^{(\rm res)}_{D^0\ell^+\ell^-}$ for the ground state (π^0, η, η') and resonance contributions.

There is little known regarding the $P_n\mu^+\mu^-$ ($P_n = \pi^0, \eta, \eta'$) vertices. In the following, we assume these quantities have the same flavor structure as the corresponding $P_n\gamma\gamma$ vertices described earlier,[4] and obtain the overall $P_n\mu^+\mu^-$ normalization from the measured

[4]This ensures that our expression will vanish in the limit of SU(3) flavor symmetry.

$\eta \to \mu^+\mu^-$ mode. From this we predict for the η' (960) $\to \mu^+\mu^-$ mode a branching ratio $\mathcal{B}r_{\eta'\mu^+\mu^-} \simeq 5.6 \times 10^{-7}$, well below the current bound $\mathcal{B}r_{\eta'\mu^+\mu^-} < 10^{-4}$. The ground state contribution is then

$$\begin{aligned} B^{(\rm gnd)}_{D^0\ell^+\ell^-} &= -\frac{G_F a_2 f_D B_{P\mu^+\mu^-}}{\sqrt{2}}\Big[\frac{\xi_d}{\sqrt{2}}\frac{M_\pi^2}{M_D^2-M_\pi^2} \\ &+\frac{2\xi_s-\xi_d}{3\sqrt{2}}\frac{M_\eta^2}{M_D^2-M_\eta^2}\left(\cos^2\theta - 2\sqrt{2}\sin\theta\cos\theta\right) \\ &+\frac{2\xi_s-\xi_d}{3\sqrt{2}}\frac{M_\eta'^2}{M_D^2-M_\eta'^2}\left(\sin^2\theta + 2\sqrt{2}\sin\theta\cos\theta\right)\Big] \ , \end{aligned} \tag{53}$$

with $B_{P\mu^+\mu^-} = 3.47 \times 10^{-5}$. This leads to the branching ratio

$$\mathcal{B}r^{(\rm gnd)}_{D^0\to\ell^+\ell^-} \ \simeq \ 2.5 \times 10^{-18} \ . \tag{54}$$

There can also, in principle, be intermediate state contributions from $J^P = 0^\pm$ neutral resonances $\{R^0\}$. Using the D^0-to-R^0 mixing amplitude already obtained in Eq. (42) and again identifying the resonance R^0 as $\pi(1800)$, we find

$$\mathcal{B}r^{(\pi(1800))}_{D^0\to\ell^+\ell^-} \ \simeq \ 1.8 \times 10^{-3}\frac{\Gamma_{\pi(1800)\ell^+\ell^-}}{M_{\pi(1800)}} \ = \ 1.8 \times 10^{-3}\mathcal{B}r_{\pi(1800)\to\ell^+\ell^-} \tag{55}$$

Upon assuming $\mathcal{B}r_{\pi(1800)\to\ell^+\ell^-} = 10^{-12}$ as our default branching ratio, we obtain

$$\mathcal{B}r^{(\pi(1800))}_{D^0\to\ell^+\ell^-} \ \simeq \ 5.0 \times 10^{-17}\frac{\mathcal{B}r_{\pi(1800)\to\ell^+\ell^-}}{10^{-12}} \ . \tag{56}$$

Although possibly enhanced relative to the light-meson pole contributions, the result is still unmeasureably small.

The Two-photon Unitarity Contribution

In the $K_L \to e^+e^-$ transition, the two-photon intermediate state is known to play an important role. Let us therefore consider the contribution of this intermediate state for $D^0 \to \ell^+\ell^-$,

$$\mathcal{I}m\ \mathcal{M}_{D^0\to\ell^+\ell^-} \ = \ \frac{1}{2!}\sum_{\lambda_1,\lambda_2}\int\frac{d^3q_1}{2\omega_1(2\pi)^3}\ \frac{d^3q_2}{2\omega_2(2\pi)^3} \tag{57}$$

$$\times\ \mathcal{M}_{D\to\gamma\gamma}\ \mathcal{M}^*_{\gamma\gamma\to\ell^+\ell^-}(2\pi)^4\delta^{(4)}(p-q_1-q_2) \ . \tag{58}$$

Upon inserting the general form of the $D^0 \to \gamma\gamma$ appearing in Eq.(30), we obtain

$$\mathcal{I}m\ A^{(\gamma\gamma)}_{D^0\ell^+\ell^-} = \alpha m_\ell B_{D^0\gamma\gamma}\ln\frac{M_D^2}{m_\ell^2} \ , \qquad \mathcal{I}m\ B^{(\gamma\gamma)}_{D^0\ell^+\ell^-} = i\alpha m_\ell C_{D^0\gamma\gamma}\ln\frac{M_D^2}{m_\ell^2} \ . \tag{59}$$

We find

$$\mathcal{B}r^{(\gamma\gamma)}_{D^0\to\mu^+\mu^-} \ \simeq \ 2.7 \times 10^{-5}\mathcal{B}r_{D^0\to\gamma\gamma} \ . \tag{60}$$

Summary of $D^0 \to \mu^+\mu^-$

The largest of our estimates, the two-photon unitarity component, for the long distance contribution to $D^0 \to \mu^+\mu^-$ favors a branching ratio somewhere in excess of 10^{-13}. More generally, it scales as 2.7×10^{-5} times the branching ratio for $D^0 \to \gamma\gamma$. With the estimate $\mathcal{B}r_{D^0\to\gamma\gamma} \geq 10^{-8}$ arrived at in the previous section, we therefore anticipate a branching ratio for $D^0 \to \mu^+\mu^-$ of at least 3×10^{-13}.

3 Potential for New Physics Contributions

As discussed in the introduction, the charm system provides a unique laboratory to probe physics beyond the Standard Model as it offers a complementary probe of physics to that attainable from a study of rare processes in the down-quark sector. As we found in the previous section, short distance SM contributions to rare charm decays are quite small due to the effectiveness of the GIM mechanism, and most reactions are dominated by long range effects. However, we saw that for some reactions there exists a window for the potential observation of new short distance effects, in particular for specific regions of the invariant dilepton mass spectrum in $D \to X\ell^+\ell^-$. Indeed in some cases, it is precisely because the SM rates are so small that charm provides an untapped opportunity to discover new effects and offers a detailed test of the SM in the up-quark sector.

In this section, we delineate some new physics possibilities, motivated by supersymmetric, grand-unified, extra dimensional, or strongly coupled extensions of the SM, which give rise to observable effects in rare charm transitions. In some cases, we find that present experimental limits on these channels already constrain the model parameter space.

3.1 Supersymmetry and Rare Charm Decays

We first examine the effects of Supersymmetry (SUSY) in rare charm decays, concentrating on the exclusive modes $D \to \pi\ell^+\ell^-$ and $D \to \rho\ell^+\ell^-$. Weak scale Supersymmetry is a possible solution to the hierarchy problem and as such is a well motivated theory of physics beyond the SM. We consider the general case of the unconstrained version of the Minimal Supersymmetric extension of the Standard Model where no particular SUSY breaking mechanism is assumed and investigate the two scenarios where R-parity is conserved or violated. Imposing the constraints on the SUSY parameter space from current data, we find that in both cases, the supersymmetric contributions to these decay channels can be quite large, particularly in the low dilepton mass region (*i.e.* below m_ρ).

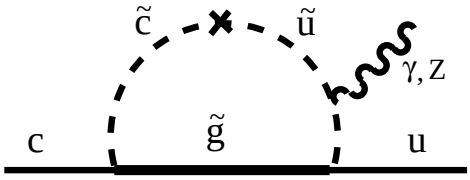

Figure 9: A typical contribution to $c \to u$ FCNC transitions in the MSSM. The cross denotes one mass insertion $(\delta^u_{12})_{\lambda\lambda'}$, with $\lambda, \lambda' = L, R$.

3.1.1 Minimal Supersymmetric Standard Model

The Minimal Supersymmetric Standard Model (MSSM) is the simplest supersymmetric extension of the SM and involves a doubling of the particle spectrum by putting all SM fermions in chiral supermultiplets, as well as the SM gauge bosons in vector supermultiplets. In our discussion, we do not assume any particular Supersymmetry breaking mechanism, but rather use a parameterization of all possible soft SUSY breaking terms. A large number, of order 100, of new parameters is then introduced. The soft supersymmetry breaking sector generally includes three gaugino masses, as well as trilinear scalar interactions, Higgs and sfermion masses. Supersymmetry contains many potential sources for flavor violation. In particular, if we choose to rotate the squark fields by the same matrices that diagonalize the quark mass matrices, then the squark mass matrices are not diagonal. In this super-CKM basis, squark propagators can be expanded so that non-diagonal mass terms result in mass insertions that change the squark flavor [29,30]. These mass insertions can be parameterized in a model independent fashion via

$$(\delta^u_{ij})_{\lambda\lambda'} = \frac{(M^u_{ij})^2_{\lambda\lambda'}}{M^2_{\tilde{q}}}\,, \tag{61}$$

where $i \neq j$ are generation indices, λ, λ' denote the chirality, $(M^u_{ij})^2$ are the off-diagonal elements of the up-type squark mass matrix, and $M_{\tilde{q}}$ represents the average squark mass. The exchange of squarks in loops thus leads to FCNC through diagrams such as the one depicted in Fig. 9. This source of flavor violation can be avoided in specific SUSY breaking scenarios such as gauge-mediation or anomaly mediation, but is present in general. It appears, for instance if SUSY breaking is mediated by gravity.

The MSSM contributions to loop mediated processes in addition to those of the SM are: gluino-squark exchange, chargino/neutralino-squark exchange and charged Higgs-quark exchange. This last contribution carries the same CKM structure as in the SM loop diagram and is proportional to the internal and external quark masses; it thus leads to small effects in rare charm transitions and we neglect it here. The gluino-squark contribution proceeds via flavor diagonal vertices proportional to the strong coupling constant and in principle dominates the CKM suppressed, weak-scale strength chargino/neutralino-squark contributions. We thus only consider the case of gluino-squark exchange here as an estimate of the potential size of supersymmetric effects in rare charm decays. We note

that the analogous gluino contributions to rare K and B transitions have led to strong universality constraints on the charged $Q = -1/3$ squark sector [31]. Here, we examine the level at which the corresponding constraints can be obtained in the charged $Q = +2/3$ squark sector once data accumulates at B and charm factories.

Within the context of the mass insertion approximation the effects are included in the Wilson coefficients corresponding to the decay $D \to X\ell^+\ell^-$ via

$$C_i = C_i^{SM} + C_i^{\tilde{g}} \,, \tag{62}$$

for $i = 7, 9, 10$. Allowing for only one insertion, the explicit contributions from the gluino-squark diagrams are [32,33]

$$C_7^{\tilde{g}} = -\frac{8}{9}\frac{\sqrt{2}}{G_F M_{\tilde{q}}^2}\pi\alpha_s \left\{ (\delta_{12}^u)_{LL}\frac{P_{132}(u)}{4} + (\delta_{12}^u)_{LR}P_{122}(u)\frac{M_{\tilde{g}}}{m_c}\right\} \,, \tag{63}$$

and

$$C_9^{\tilde{g}} = -\frac{8}{27}\frac{\sqrt{2}}{G_F M_{\tilde{q}}^2}\pi\alpha_s \,(\delta_{12}^u)_{LL}P_{042}(u) \,, \tag{64}$$

with the contribution to C_{10} vanishing at this order due to the helicity structure. If we allow for two mass insertions, there is a contribution to $C_{9,10}$ given by

$$C_{10}^{\tilde{g}} = -\frac{1}{9}\frac{\alpha_s}{\alpha}\,(\delta_{22}^u)_{LR}(\delta_{12}^u)_{LR}P_{032}(u) = -\frac{C_9}{1-4\sin^2\theta_W} \,. \tag{65}$$

Here, $u = M_{\tilde{g}}^2/M_{\tilde{q}}^2$ and the functions $P_{ijk}(u)$ are defined as

$$P_{ijk}(u) \equiv \int_0^1 dx\, \frac{x^i(1-x)^j}{(1-x+ux)^k} \,. \tag{66}$$

In addition, the operator basis can be extended by the "wrong chirality" operators $\hat{O}_7$, $\hat{O}_9$ and $\hat{O}_{10}$, obtained by switching the quark chiralities in Eqs. (6) and (7). The gluino-squark contributions to the corresponding Wilson coefficients are

$$\begin{aligned}
\hat{C}_7^{\tilde{g}} &= -\frac{8}{9}\frac{\sqrt{2}}{G_F M_{\tilde{q}}^2}\pi\alpha_s \left\{ (\delta_{12}^u)_{RR}\frac{P_{132}(u)}{4} + (\delta_{12}^u)_{LR}P_{122}(u)\frac{M_{\tilde{g}}}{m_c}\right\} \,, \qquad (67)\\
\hat{C}_9^{\tilde{g}} &= -\frac{8}{27}\frac{\sqrt{2}}{G_F M_{\tilde{q}}^2}\pi\alpha_s \,(\delta_{12}^u)_{RR}P_{042}(u) - (1-4\sin^2\theta_W)\hat{C}_{10}^{\tilde{g}} \,,\\
\hat{C}_{10}^{\tilde{g}} &= -\frac{1}{9}\frac{\alpha_s}{\alpha}\,(\delta_{22}^u)_{LR}(\delta_{12}^u)_{LR}P_{032}(u) \quad ,
\end{aligned}$$

where the expression for $\hat{C}_{10}^{\tilde{g}}$ is again obtained with a double insertion.

As was noted in Refs. [32,33], in both $C_7^{\tilde{g}}$ and $\hat{C}_7^{\tilde{g}}$ the term in which the squark chirality labels are mixed introduces the enhancement factor $M_{\tilde{g}}/m_c$. In the SM the chirality flip

which appears in O_7 occurs by a flip of one external quark line, resulting in a factor of m_c included in the operator's definition[5]. However, in the gluino-squark diagram, the insertion of $(\delta^u_{12})_{RL}$ forces the chirality flip to take place in the gluino line, thus introducing a $M_{\tilde{g}}$ factor instead of m_c. This yields a significant enhancement in the short distance contributions to the process $D \to X_u\gamma$ [33], which is unfortunately obscured by the large long range effects.

The most stringent bounds that apply to the non-universal soft breaking terms $(\delta^u_{12})_{\lambda\lambda'}$ come from the experimental searches for $D^0 - \bar{D}^0$ mixing[6]. The current CLEO limit [8] implies [33]

$$\frac{1}{2}\left\{\left(\frac{\Delta m_D}{\Gamma_{D^0}}\right)^2 \cos\delta + \left(\frac{\Delta\Gamma_D}{2\Gamma_{D^0}}\right)^2 \sin\delta\right\} < 0.04\% \ , \tag{68}$$

where δ is a strong relative phase between the Cabibbo-allowed and the doubly Cabibbo-suppressed $D^0 \to K\pi$ decays. Neglecting this phase results in the constraints obtained in Ref. [33], which we collect in Table 3. These bounds were obtained assuming that

$M^2_{\tilde{g}}/M^2_{\tilde{q}}$	$(\delta^u_{12})_{LL}$	$(\delta^u_{12})_{LR}$
0.3	0.03	0.04
1.0	0.06	0.02
4.0	0.14	0.02

Table 3: Bounds on $(\delta^u_{12})_{LL}$, $(\delta^u_{12})_{LR}$ from $D^0 - \bar{D}^0$ mixing [33] (neglecting the strong phase). All constraints should be multiplied by $(M_{\tilde{q}}/500$ GeV).

$(\delta^u_{12})_{RR} = 0$ and $(\delta^u_{12})_{LR} = (\delta^u_{12})_{RL}$; these assumptions are found to be numerically unimportant.

In order to estimate the effects in $c \to u\ell^+\ell^-$ transitions from the gluino contributions, we need to specify $M_{\tilde{g}}$ and $M_{\tilde{q}}$. We consider four sample cases: (I): $M_{\tilde{g}} = M_{\tilde{q}} = 250$ GeV; (II): $M_{\tilde{g}} = 2\,M_{\tilde{q}} = 500$ GeV; (III): $M_{\tilde{g}} = M_{\tilde{q}} = 1000$ GeV and (IV): $M_{\tilde{g}} = (1/2)\,M_{\tilde{q}} = 250$ GeV. We first examine $D^+ \to \pi^+e^+e^-$. In Fig. 10 we show the dilepton mass distribution as a function of the dilepton mass. Although the net effect is relatively small in the integrated rate (an increase $\simeq 20\%$ or smaller), the enhancement due to the SUSY contributions is most conspicuous away from the vector resonances, particularly for low dilepton masses. Experiments sensitive to the dilepton mass distribution at the level of $10^{-7} - 10^{-8}$ can detect these SUSY contributions. However, the decays to a vector meson, such as $D \to \rho e^+e^-$, are more sensitive to the gluino exchange, as can be seen from

[5] The m_u term, proportional to the $(1-\gamma_5)$ in the operator, is neglected.

[6] Limits obtained from charge and color breaking (CCB) and bounding the potential from below (UFB) [34] apply to the trilinear terms but not to the squark mass terms. Thus, unless the squark mass matrices are kept diagonal, CCB and UFB arguments cannot be used to constrain the non-universal mass insertions.

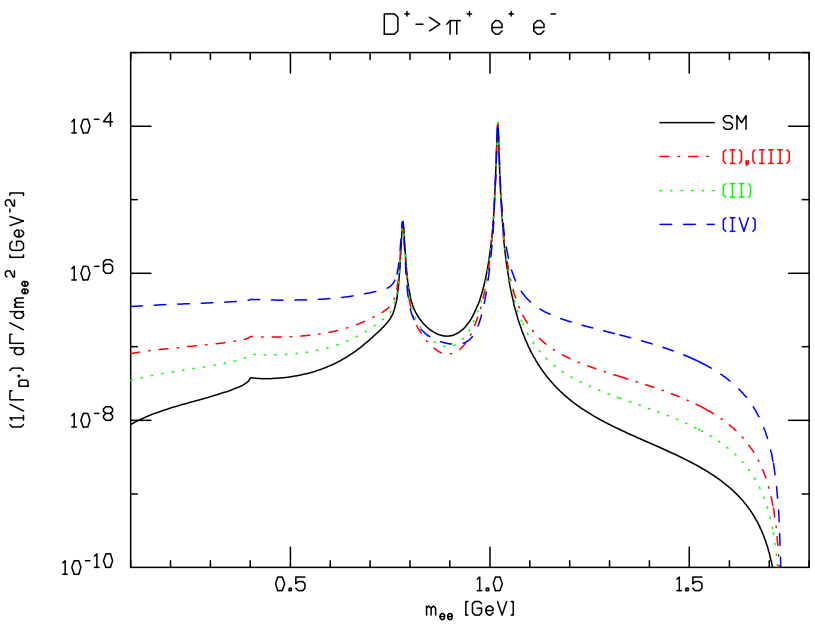

Figure 10: The dilepton mass distribution for $D^+ \to \pi^+ e^+ e^-$ (normalized to Γ_{D^+}), in the MSSM with non-universal soft breaking effects. The solid line is the SM; (I): $M_{\tilde{g}} = M_{\tilde{q}} = 250$ GeV; (II): $M_{\tilde{g}} = 2\, M_{\tilde{q}} = 500$ GeV; (III): $M_{\tilde{g}} = M_{\tilde{q}} = 1000$ GeV and (IV): $M_{\tilde{g}} = (1/2)\, M_{\tilde{q}} = 250$ GeV.

Fig. 11. The effect is quite pronounced and almost entirely lies in the low m_{ee} region. This is mostly due to the contributions of $(\delta^u_{12})_{RL}$ to C_7 and $\hat{C}_7$ in Eqs. (63) and (67), which contain the $M_{\tilde{g}}/m_c$ enhancement as discussed above. This effect is intensified at low $q^2 = m^2_{ee}$ due to the photon propagator (see for instance Eq. (12) for the inclusive decays). This low q^2 enhancement of the O_7 contribution is present in exclusive modes with vector mesons such as $D \to \rho \ell^+ \ell^-$, but not in modes with pseudoscalars, such as $D \to \pi \ell^+ \ell^-$, since gauge invariance forces a cancellation of the $1/q^2$ factor in the latter case (*e.g.*, see Eq. (15)). This is apparent from a comparison of the low dilepton mass regions in Figs. (10) and (11).

We conclude that the $D \to \rho \ell^+ \ell^-$ decays are considerably sensitive to non-universal soft breaking in the MSSM. The largest effect is obtained in case (IV) (dashed line in Fig. (11)) and yields $\mathcal{B}r_{D^0 \to \rho^0 e^+ e^-} \simeq 1.3 \times 10^{-5}$, which is roughly a factor of five times larger than the SM prediction given in Sect. 2.1.2. The current experimental bound on this channel is [35] $\mathcal{B}r^{\rm exp}_{D^0 \to \rho^0 e^+ e^-} < 1.2 \times 10^{-4}$. For muon final states, the somewhat more stringent constraint $\mathcal{B}r^{\rm exp}_{D^0 \to \rho^0 \mu^+ \mu^-} < 2.2 \times 10^{-5}$ should be compared to $\mathcal{B}r_{D^0 \to \rho^0 \mu^+ \mu^-} \simeq 1.3 \times 10^{-6}$ obtained in case (IV). Thus, searches for rare charm decays with sensitivities of 10^{-6} and better will soon constrain the MSSM parameter space or observe an effect.

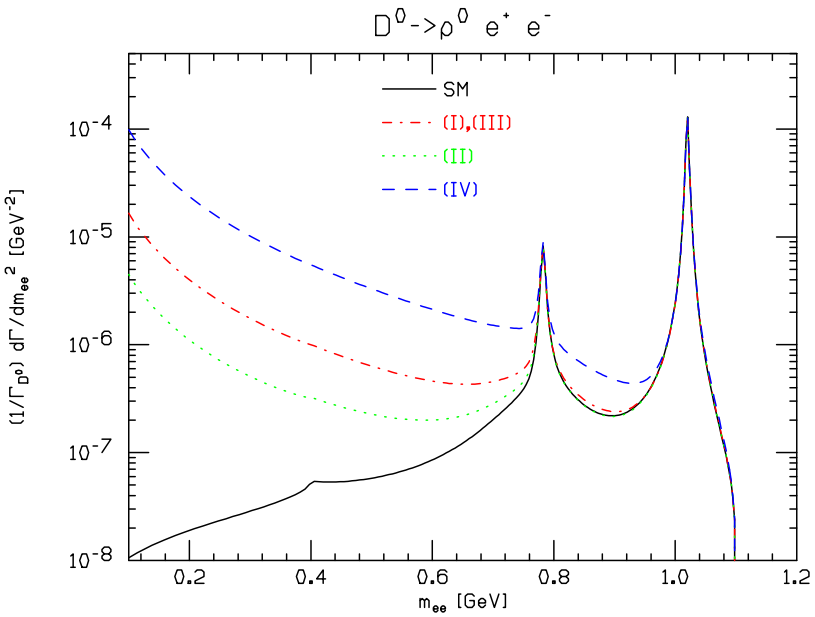

Figure 11: The dilepton mass distribution for $D^0 \to \rho^0 e^+ e^-$ (normalized to Γ_{D^0}), in the MSSM with non-universal soft breaking effects. The solid line is the SM; (I): $M_{\tilde{g}} = M_{\tilde{q}} = 250$ GeV; (II): $M_{\tilde{g}} = 2\,M_{\tilde{q}} = 500$ GeV; (III): $M_{\tilde{g}} = M_{\tilde{q}} = 1000$ GeV and (IV): $M_{\tilde{g}} = (1/2)\,M_{\tilde{q}} = 250$ GeV.

3.1.2 R Parity Violation

The assumption of R-parity conservation in the MSSM prohibits baryon and lepton number violating terms in the super-potential. However, other symmetries can be invoked to prohibit rapid proton decay, such as baryon-parity or lepton-parity [36], and hence allow for R parity violation. The R-parity violating super-potential can be written as[7]

$$\mathcal{W}_{R_p} = \epsilon_{ab}\left\{\frac{1}{2}\lambda_{ijk}L_i^a L_j^b \bar{E}_k + \lambda'_{ijk}L_i^a Q_j^b \bar{D}_k + \frac{1}{2}\epsilon_{\alpha\beta\gamma}\lambda''_{ijk}\bar{U}_i^\alpha \bar{D}_j^\beta \bar{D}_k^\gamma\right\}\,, \tag{69}$$

where L, Q, $\bar{E}$, $\bar{U}$ and $\bar{D}$ are the chiral super-fields in the MSSM. The $SU(3)$ color indices are denoted by $\alpha, \beta, \gamma = 1, 2, 3$, the $SU(2)_L$ indices by $a, b = 1, 2$ and the generation indices are $i, j, k = 1, 2, 3$. The fields in Eq. (69) are in the weak basis. The λ'_{ijk} term is the one which is relevant for the rare charm decays we consider here as it can give rise to tree-level contributions through the exchange of squarks to decay channels such as $D \to X\ell^+\ell^-$, $D \to \ell^+\ell^-$, as well as the lepton-flavor violating $D \to X\mu^+e^-$ and $D \to \mu^+e^-$ modes. Before considering the FCNC effects in D decays, we need to rotate the fields to the mass basis. This leads to

$$\mathcal{W}_{R_p} = \tilde{\lambda}'_{ijk}\left[N_i V_{jl} D_l - E_i U_j\right]\bar{D}_k + \cdots \tag{70}$$

[7]We ignore bilinear terms which are not relevant to our discussion of FCNC effects.

where V is the CKM matrix and we define

$$\tilde{\lambda'}_{ijk} \equiv \lambda'_{irs}\mathcal{U}^L_{rj}\mathcal{D}^{*R}_{sk} \ . \tag{71}$$

Here, $\mathcal{U}^L$ and $\mathcal{D}^R$ are the matrices used to rotate the left-handed up- and right-handed down-quark fields to the mass basis. Written in terms of component fields, this interaction now reads

$$\begin{aligned}\mathcal{W}_{\lambda'} &= \tilde{\lambda}'_{ijk}\Big\{V_{jl}[\tilde{\nu}^i_L\bar{d}^k_R d^l_L + \tilde{d}^l_L\bar{d}^k_R\nu^i_L + (\tilde{d}^k_R)^*(\bar{\nu^i_L})^c d^l_L] \\ &\quad -\tilde{e}^i_L\bar{d}^k_R u^j_L - \tilde{u}^j_L\bar{d}^k_R e^i_L - (\tilde{d}^k_R)^*(\bar{e^i_L})^c u^j_L\Big\} \ . \end{aligned} \tag{72}$$

The last term in Eq. (72) can give rise to the processes $c \to u\ell\ell^{(\prime)}$ at tree level via the exchange of a down-squark. This leads to effects that are proportional to $\tilde{\lambda}'_{i2k}\tilde{\lambda}'_{i1k}$ with $i = 1, 2$ (due to kinematical restrictions).

Constraints on these coefficients have been derived in the literature [37]. For instance, tight bounds are obtained in Ref. [38] from $K^+ \to \pi^+\nu\bar{\nu}$ by assuming that only one R-parity violating coupling satisfies $\tilde{\lambda}'_{ijk} \neq 0$. We update this bound by using the latest experimental result [39] $\mathcal{B}r_{K^+\to\pi^+\nu\bar{\nu}} = (1.57^{+1.75}_{-0.82}) \times 10^{-10}$, which yields $\tilde{\lambda}'_{ijk} < 0.005$. However, this bound can be avoided in the single coupling scheme [38], where only one R-parity violating coupling is taken to be non-zero in the weak basis. In this case, it is possible that flavor rotations may restrict the R-parity breaking induced flavor violation to be present in either the charge $-1/3$ or $+2/3$ quark sectors, but not both. Then large effects are possible in the up sector for observables such as D^0-$\bar{D}^0$ mixing and rare decays without affecting the down-quark sector. In Ref. [38] a rather loose constraint on the R-parity breaking couplings is obtained from D^0 mixing, which could result in large effects in $c \to u\ell\ell^{(\prime)}$ decays. Here, we will take a conservative approach and make use of more model-independent bounds. The constraints on the R-parity breaking couplings for the processes of interest here are collected in Table 4 from Ref. [37]. The charged current universality bounds assume three generations. The π decay constraint is given by the quantity $R_\pi = \Gamma_{\pi\to e\nu}/\Gamma_{\pi\to\mu\nu}$. The limits obtained from $D \to K\ell\nu$ were first obtained in Ref. [40].

$\tilde{\lambda}'_{11k}$	$\tilde{\lambda}'_{12k}$	$\tilde{\lambda}'_{21k}$	$\tilde{\lambda}'_{22k}$
$0.02^{(a)}$	$0.04^{(a)}$	$0.06^{(b)}$	$0.21^{(c)}$

Table 4: Most stringent (2σ) bounds for the R-parity violation couplings entering in rare D decays, from (a) charged current universality, (b) R_π and (c) $D \to K\ell\nu$. See Ref. [37] for details. All numbers should be multiplied by $(m_{\tilde{d}^k_R}/100$ GeV).

We first consider the contributions to $c \to u\ell^+\ell^-$. The tree level exchange of down squarks results in the effective interaction

$$\delta\mathcal{H}_{\rm eff} = -\frac{\tilde{\lambda}'_{i2k}\tilde{\lambda}'_{i1k}}{m^2_{\tilde{d}^k_R}}\,\overline{(\ell_L)^c}c_L\;\bar{u}_L(\ell_L)^c\;, \tag{73}$$

which after Fierzing gives

$$\delta\mathcal{H}_{\rm eff} = -\frac{\tilde{\lambda}'_{i2k}\tilde{\lambda}'_{i1k}}{2m^2_{\tilde{d}^k_R}}\,(\bar{u}_L\gamma_\mu c_L)(\bar{\ell}_L\gamma^\mu\ell_L)\;. \tag{74}$$

This corresponds to contributions to the Wilson coefficients C_9 and C_{10} at the high energy scale given by

$$\delta C_9 = -\delta C_{10} = \frac{\sin^2\theta_W}{2\alpha^2}\left(\frac{M_W}{m_{\tilde{d}^k_R}}\right)^2\tilde{\lambda}'_{i2k}\tilde{\lambda}'_{i1k}\;. \tag{75}$$

If we now specify $\ell = e$ and use the bounds from Table 4 we arrive at the constraint

$$\delta C_9^e = -\delta C_{10}^e \leq 1.10\left(\frac{\tilde{\lambda}'_{12k}}{0.04}\right)\left(\frac{\tilde{\lambda}'_{11k}}{0.02}\right)\;. \tag{76}$$

Notice that these are independent of the squark mass, which cancels. Taking this upper limit on the Wilson coefficients results in the dot-dashed lines of Figs. 1 and 2 corresponding to $D^+ \to \pi^+e^+e^-$ and $D^0 \to \rho^0e^+e^-$, respectively. The effect in these rates is small, of order 10% at most, whereas the experimental bounds are a factor of 20 above this level in the best case (given by the pion mode).

On the other hand, for $\ell = \mu$ we obtain

$$\delta C_9^\mu = -\delta C_{10}^\mu \leq 17.4\left(\frac{\tilde{\lambda}'_{22k}}{0.21}\right)\left(\frac{\tilde{\lambda}'_{21k}}{0.06}\right)\;. \tag{77}$$

These upper limits already saturate the experimental bounds of $\mathcal{B}r^{\rm exp}_{D^+\to\pi^+\mu^+\mu^-} < 1.5\times10^{-5}$ and $\mathcal{B}r^{\rm exp}_{D^0\to\rho^0\mu^+\mu^-} < 2.2\times10^{-5}$ from Refs. [35,41]! Thus we derive the following new constraint on the product of R-parity violating couplings,

$$\tilde{\lambda}'_{22k}\,\tilde{\lambda}'_{21k} < 0.004\;\;, \tag{78}$$

which arises from the $D^+ \to \pi^+\mu^+\mu^-$ mode. This allows for potentially large effects in both the ρ and π channels as is illustrated in Figs. 12 and 13.

In Figure 12 we display the dimuon mass distribution as a function of the dimuon mass for $D^+ \to \pi^+\mu^+\mu^-$. The solid line, corresponding to the SM prediction and including both the short and long distance pieces, is clearly dominated by the latter through the presence of the vector meson resonances as discussed above. The dashed line includes the

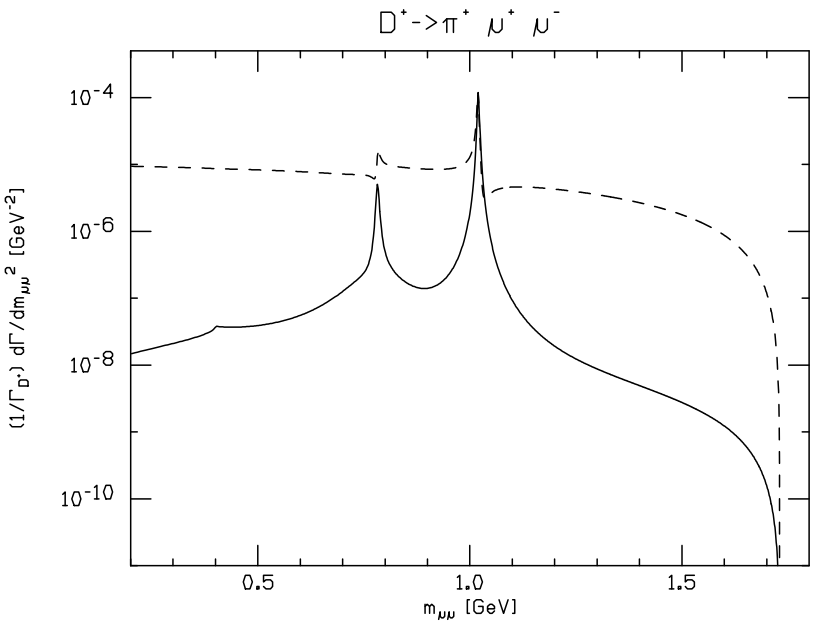

Figure 12: The dilepton mass distribution for $D^+ \to \pi^+\mu^+\mu^-$ normalized to Γ_{D^+}. The solid line shows the sum of the short and the long distance SM contributions. The dashed line includes the allowed R-parity violating contribution from Supersymmetry (see text for details).

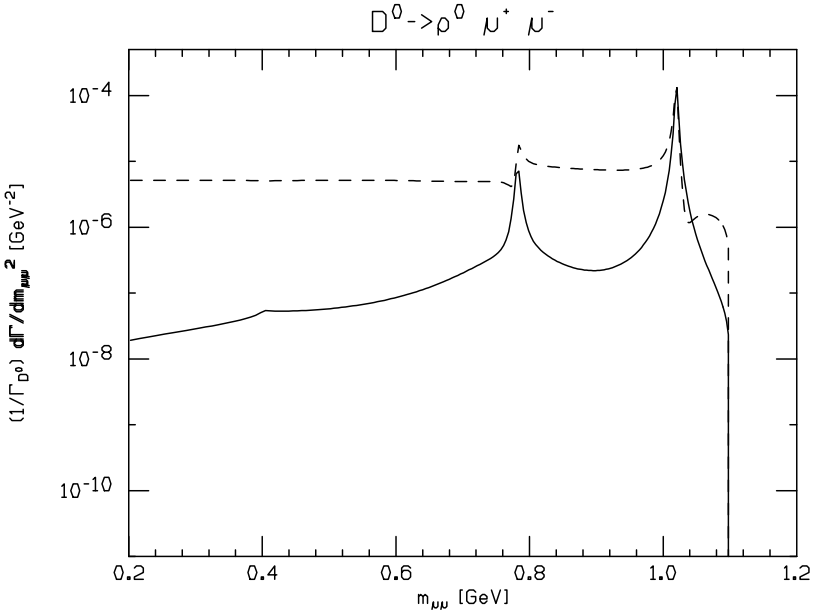

Figure 13: The dilepton mass distribution for $D^0 \to \rho^0\mu^+\mu^-$ normalized to Γ_{D^0}. The solid line shows the sum of the short and the long distance SM contributions. The dashed line includes the allowed R-parity violating contribution from Supersymmetry (see text for details).

contribution of R parity violation, taking the R-parity violating coefficients to saturate the above bound in Eq. (78). It can be seen that *away from the resonances* there is an important window for the discovery of R parity violation in SUSY theories. The situation is similar in the $D^0 \to \rho^0 \mu^+ \mu^-$ distribution, shown in Figure 13. Here, the dashed line is again obtained by making use of the bound in Eq. (78). This results in an upper bound for the R parity violating effect given by $\mathcal{B}r^{R_{\not P}}_{D^0 \to \rho^0 \mu^+ \mu^-} < 8.7 \times 10^{-6}$, which is still below the experimental limit [41] $\mathcal{B}r^{\rm exp}_{D^0 \to \rho^0 \mu^+ \mu^-} < 2.2 \times 10^{-5}$.

In addition to the dilepton mass distribution, this decay mode also contains angular information as discussed in the previous section. For instance, we can define the forward-backward asymmetry for leptons as

$$A_{FB}(q^2) = \frac{\int_0^1 \frac{d^2\Gamma}{dx dq^2} dx - \int_{-1}^0 \frac{d^2\Gamma}{dx dq^2} dx}{\frac{d\Gamma}{dq^2}} \quad , \tag{79}$$

where $x \equiv \cos\theta$, with θ being the angle between the ℓ^+ and the decaying D meson in the $\ell^+\ell^-$ rest frame. Expressions for the angular distribution $d\Gamma/dxdq^2$ can be found in Ref. [42] for the inclusive case and in Ref. [43,44] for the exclusive modes. In the SM, $A_{FB}(q^2)$ in $D^0 \to \rho^0 \ell^+ \ell^-$ is negligibly small throughout the kinematic region. The reason for this can be seen by inspecting the numerator of the asymmetry [43]

$$A_{FB}(q^2) \sim 4\, m_D\, k\, C_{10} \left\{ C_9^{\rm eff}\; g\; f + \frac{m_c}{q^2} C_7^{\rm eff}\; (f\; G - g\; F) \right\} \; , \tag{80}$$

where k is the vector meson three-momentum in the D rest frame, and f, g, F and G are various form-factors. Since the SM amplitude is dominated by the long distance vector intermediate states, we have $C_9^{\rm eff} \gg C_{10}$. New physics contributions that make $C_{10} \simeq C_9^{\rm eff}$ will hence generate a sizable asymmetry. This is illustrated in the case at hand of R parity violating supersymmetry. For instance, again setting the coupling to the values given in Eq. (78), we present the forward-backward asymmetry for $D^0 \to \rho^0 \mu^+ \mu^-$ in Figure 14. In order to compute the asymmetry, we make use of $D^0 \to K^* \ell \nu$ form-factors, together with $SU(3)$ symmetry and heavy quark *spin* symmetry[8]. This gives a bound on the integrated asymmetry of $I_{FB}^{\mu\mu} \simeq 0.15$. For $D^0 \to \rho^0 e^+ e^-$, we get $I_{FB}^{ee} \simeq 0.08$. Supersymmetry could thus produce very sizable asymmetries. In general, any non-zero value of $A_{FB}(q^2)$ that is measured should be interpreted as arising from new physics.

The effective interactions of Eq. (73) also lead to a contribution to the two body decay $D^0 \to \mu^+ \mu^-$. The R parity violating contribution to the branching ratio then reads

$$\mathcal{B}r^{\not R_p}_{D^0 \to \mu^+ \mu^-} = \tau_{D^0}\, f_D^2\, m_\mu^2\, m_D \sqrt{1 - \frac{4m_\mu^2}{m_D^2}}\; \frac{\left(\tilde{\lambda}'_{22k} \tilde{\lambda}'_{21k}\right)^2}{64\pi\, m^4_{\tilde{d}_k}} \; . \tag{81}$$

[8] See the first reference cited in Ref. [43].

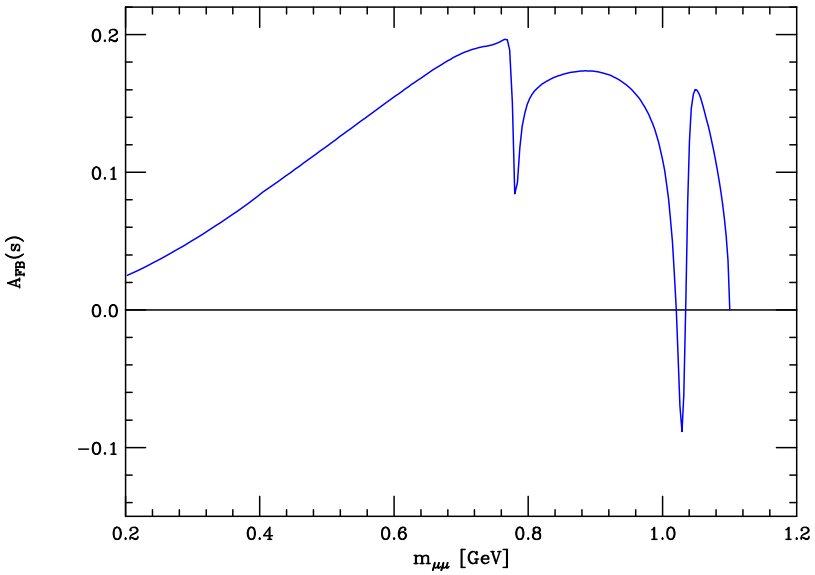

Figure 14: The lepton forward-backward asymmetry for $D^0 \to \rho^0 \mu^+ \mu^-$, for the bound of Eq. (78). (see text for details)

Applying the bound in Eq. (78) gives the constraint

$$\mathcal{B}r^{\not R_p}_{D^0 \to \mu^+ \mu^-} < 3.5 \times 10^{-6} \left(\frac{\tilde{\lambda}'_{12k}}{0.04}\right)^2 \left(\frac{\tilde{\lambda}'_{11k}}{0.02}\right)^2 . \tag{82}$$

The current experimental limit [35] $\mathcal{B}r_{D^0 \to \mu^+ \mu^-} < 5.2 \times 10^{-6}$ is just above this value, implying that future measurements of this decay mode will constrain the product of these R parity violating couplings.

Finally, we consider the products of R parity violating couplings that lead to lepton flavor violation. For instance, the products $\tilde{\lambda}'_{11k}\tilde{\lambda}'_{22k}$ and $\tilde{\lambda}'_{21k}\tilde{\lambda}'_{12k}$ will give rise to $D^+ \to \pi^+ \mu^+ e^-$. This leads to

$$\delta C_9^{\mu e} = -\delta C_{10}^{\mu e} = 4.6 \times \left\{ \left(\frac{\tilde{\lambda}'_{11k}}{0.02}\right)\left(\frac{\tilde{\lambda}'_{22k}}{0.21}\right) + \left(\frac{\tilde{\lambda}'_{21k}}{0.06}\right)\left(\frac{\tilde{\lambda}'_{12k}}{0.04}\right) \right\} , \tag{83}$$

which results in $\mathcal{B}r^{\not R_p}_{D^+ \to \pi^+ \mu^+ e^-} < 3 \times 10^{-5}$, to be contrasted with [35] $\mathcal{B}r^{\rm exp}_{D^+ \to \pi^+ \mu^+ e^-} < 3.4 \times 10^{-5}$. Here again, experiment is on the verge of being sensitive to R parity violating effects in supersymmetry. Similarly, for the corresponding two body decay we have

$$\mathcal{B}r^{\not R_p}_{D^0 \to \mu^+ e^-} < 0.5 \times 10^{-6} \times \left\{ \left(\frac{\tilde{\lambda}'_{11k}}{0.02}\right)\left(\frac{\tilde{\lambda}'_{22k}}{0.21}\right) + \left(\frac{\tilde{\lambda}'_{21k}}{0.06}\right)\left(\frac{\tilde{\lambda}'_{12k}}{0.04}\right) \right\} , \tag{84}$$

whereas the current bound is [35] $\mathcal{B}r^{\rm exp}_{D^0 \to \mu^+ e^-} < 8.1 \times 10^{-6}$. We summarize the results of this section in Table 5.

Finally, we point out that similar effects to those considered in this section are generated by leptoquarks. Their exchange lead in general to effective interactions similar to the λ' terms in Eq. (69).

Decay Mode	SM	$\not{R}_p$	Expt. Limit
$D^+ \to \pi^+ e^+ e^-$	2.0×10^{-6}	2.3×10^{-6}	5.2×10^{-5}
$D^0 \to \rho^0 e^+ e^-$	1.8×10^{-6}	5.1×10^{-6}	1.0×10^{-4}
$D^+ \to \pi^+ \mu^+ \mu^-$	1.9×10^{-6}	1.5×10^{-5}	1.5×10^{-5}
$D^0 \to \rho^0 \mu^+ \mu^-$	1.8×10^{-6}	8.7×10^{-6}	2.3×10^{-4}
$D^0 \to \mu^+ \mu^-$	3.0×10^{-13}	3.5×10^{-6}	4.1×10^{-6}
$D^0 \to e^+ e^-$	10^{-23}	1.0×10^{-10}	6.2×10^{-6}
$D^0 \to \mu^+ e^-$	0	1.0×10^{-6}	8.1×10^{-6}
$D^+ \to \pi^+ \mu^+ e^-$	0	3.0×10^{-5}	3.4×10^{-5}
$D^0 \to \rho^0 \mu^+ e^-$	0	1.4×10^{-5}	4.9×10^{-5}

Table 5: Comparison of various decay modes between the SM and R parity violation. The third column shows how large the R parity violating effect can be. The experimental limits are from Refs. [16],[35],[41].

3.2 Extensions of Standard Model with Extra Higgses, Gauge Bosons, Fermions, or Dimensions

In this section we summarize the results from classes of models which have additional Higgs scalar doublets, or family gauge symmetry or extra leptons. All of these give rise to flavor changing couplings at tree level and hence yield potentially large rates for rare decay modes of D mesons. In addition we briefly discuss the effects of extra dimensional physics on rare charm transitions.

3.2.1 Multiple Higgs Doublets

Many extensions of the Standard Model contain more than one Higgs scalar doublet. As is well known, this leads in general to tree level FCNC couplings and thus decays such as $D^0 \to \mu^+\mu^-, e^+e^-, \mu^\pm e^\mp$, *etc* may proceed at rates larger than SM expectations. In the down quark sector, there are severe constraints on such couplings from kaon decay modes [45]. This does not necessarily lead to equally strong constraints on the up-quark sector. For example, as was shown long ago [46], it is possible that simple symmetries forbid $\Delta S = 1$ FCNC without affecting the $\Delta C = 1$ sector.

Let us write the general effective $\Delta C = 1$ interaction as

$$\beta \frac{G_F}{\sqrt{2}} \; \bar{u}\gamma_5 c \; \bar{\ell}_1 (a + b\gamma_5)\ell_2 \quad , \tag{85}$$

where β is a model dependent dimensionless number, a and b refer to generic scalar and pseudoscalar couplings, respectively, and ℓ_1, ℓ_2 refer to the pairs (μ, μ), (e, e) or (μ, e). Comparing to the mode $D^+ \to \mu^+ \nu_\mu$, one can write

$$\begin{aligned} \mathcal{B}r_{D^0 \to \ell_1 \bar{\ell}_2} &\cong \frac{\beta^2}{\mid U_{cd} \mid^2} \frac{m_D^2}{m_c m_\mu} \frac{a^2 + b^2}{2} \frac{\tau_D^+}{\tau_D^0} \; \mathcal{B}r_{D^+ \to \mu^+ \nu} \\ &\cong 11.35 \; \beta^2 \frac{a^2 + b^2}{2} \quad . \end{aligned} \tag{86}$$

The corresponding branching ratio for the three body modes $c \to u l_i l_j$ is given by $0.343 \beta^2 \left(a^2 + b^2\right)/2$.

We have evaluated the parameters β, a and b in several models with multiple Higgs scalar doublets [46],[47] and computed the branching ratios for rare decay modes of the D^0. We find that the branching ratios for these modes can be as large as

$$\mathcal{B}r_{D^0 \to \mu^+ \mu^-} \sim 8 \times 10^{-10} \; , \qquad \mathcal{B}r_{D^0 \to e^+ e^-} \sim 4 \times 10^{-14} \; , \qquad \mathcal{B}r_{D^0 \to \mu^\pm e^\mp} \sim 7 \times 10^{-10} \quad , \tag{87}$$

with the corresponding three body modes having branching ratios smaller than these by about a factor of 30. While still small, these values are greatly enhanced over those in the SM.

3.2.2 FCNC in Horizontal Gauge Models

The gauge sector in the Standard Model has a large global symmetry which is broken by the Higgs interaction. By enlarging the Higgs sector, some subgroup of this symmetry can be imposed on the full SM lagrangian and break the symmetry spontaneously. This family symmetry can be global as well as gauged [48]. If the new gauge couplings are very weak or the gauge boson masses are large, the difference between a gauged or global symmetry is rather difficult to distinguish in practice. In general there would be FCNC effects from both the gauge and scalar sectors. Here we consider the gauge contributions.

Let us construct a simple toy model as an example. Consider a family symmetry $SU(2)_H$ under which the left-handed quarks (where the superscripts denote the weak flavor eigenstates)

$$\begin{pmatrix} u^0 \\ d^0 \end{pmatrix}_L \quad \begin{pmatrix} c^0 \\ s^0 \end{pmatrix}_L ,$$

and the corresponding left-handed leptons

$$\begin{pmatrix} \nu_e^0 \\ e^0 \end{pmatrix}_L \quad \begin{pmatrix} \nu_\mu^0 \\ \mu^0 \end{pmatrix}_L ,$$

transform as members of an $I_H = 1/2$ family doublet. The third family is assumed to have $I_H = 0$. The $SU(2)_H$ symmetry in this model can be thought of as a remnant of an $SU(3)_H$ family symmetry which has been broken to $SU(2) \times U(1)$. If $\{G_\mu^i\}$ are the gauge fields corresponding to the $SU(2)_H$ and we denote $\psi_{d_L^0} = \begin{pmatrix} d^0 \\ s^0 \end{pmatrix}_L$, $\psi_{u_L^0} = \begin{pmatrix} u^0 \\ c^0 \end{pmatrix}_L$, *etc*, then the gauge interactions are

$$g \left[\bar{\psi}_{d_L^0} \ \gamma_\mu \tau \cdot \mathbf{G}^\mu \psi_{d_L^0} \ + (d^0 \to u^0) \ + (d^0 \to \ell^0) \right] \quad . \tag{88}$$

After the symmetry is broken, the mass eigenstate basis is given by

$$\begin{pmatrix} d \\ s \end{pmatrix}_L = U_d \begin{pmatrix} d^0 \\ s^0 \end{pmatrix}_L , \quad \begin{pmatrix} u \\ c \end{pmatrix}_L = U_u \begin{pmatrix} u^0 \\ c^0 \end{pmatrix}_L , \begin{pmatrix} e \\ \mu \end{pmatrix}_L = U_\ell \begin{pmatrix} e^0 \\ \mu^0 \end{pmatrix}_L . \tag{89}$$

The matrices U_u, U_d and U_ℓ each contain one angle, θ_f, and three phases. After the symmetry is broken, the three gauge bosons acquire different masses, m_i. If the phases are ignored, the matrix elements for the processes of interest are:

$$\begin{aligned} \mathcal{M}_{D^0 \to \mu^+ \mu^-} &= \frac{1}{2} g^2 f_D \ m_\mu \left[\frac{\sin \ 2\theta_u \cos \theta_e}{m_3^2} \ - \frac{\cos \ 2\theta_u \sin 2\theta_e}{m_1^2} \right] \bar{\mu}(1+\gamma_5)\mu \ , \qquad (90) \\ \mathcal{M}_{D^0 \to e^- \mu^+} &= \frac{1}{4} g^2 f_D \ m_\mu \left[\frac{\cos \ 2\theta_u \cos 2\theta_e}{m_1^2} \ + \frac{1}{m_2^2} \ + \frac{\sin 2\theta_u \sin 2\theta_e}{m_3^2} \right] \bar{\mu}(1+\gamma_5)e \ . \end{aligned}$$

Corresponding expressions exist for K^0 decay modes, with θ_d replacing θ_u. To proceed further, let us make the simplifying assumption that $m_1 \approx m_2 \ll m_3$ and that the mixing angles are small. Then, using the constraints from the kaon system, namely the bounds on $K_L \to e\mu$ and the known rate for $K_L \to \mu\bar{\mu}$, we find that the branching ratios for charm decay modes can be as large as

$$\mathcal{B}r_{D^0 \to \mu^+ \mu^-} \sim 3.10^{-10} \qquad \text{and} \qquad \mathcal{B}r_{D^0 \to \mu^\pm e^\mp} \sim 2.10^{-13} \ , \tag{91}$$

which are enhanced over the SM expectations.

3.2.3 Extra Fermions

Additional fermions beyond those in the three families of the SM can contribute to a variety of rare charm decays and can serve to remove the effective GIM cancellation inherent to these transitions in the SM. Let us first consider the effect of an SU(2) singlet

down-type Q=-1/3 quark of the kind that occurs in E_6 models [49]. This b' quark will contribute in the loop diagrams [50] which mediate decays such as $D^0 \to \mu^+\mu^-$. For a mass $m_{b'} \simeq 250$ GeV, the mixing with u and c quarks given by $\lambda_{b'} = V_{ub'}V_{cb'}^*$ is constrained by the b' contribution to Δm_D. With the current bound on x_D ($x_D \equiv \Delta m_D/\Gamma_D$) of about 3% [8], $\lambda_{b'}$ has to satisfy $\lambda_{b'} < 0.003$. The b' contribution to $D^0 \to \mu^+\mu^-$ can then be of order

$$\mathcal{B}r_{D^0\to\mu^+\mu^-}(b') \approx 10^{-11} \quad , \tag{92}$$

which is two orders of magnitude above the SM value. There will be similar enhancements for modes such as $D \to \pi\ell\bar{\ell}, D \to \rho\ell\bar{\ell}$ which would be experimentally detectable. We note that an additional fourth family down-type quark belonging to a $SU(2)_L$ doublet would have an identical effect.

When the SM is extended by adding extra lepton doublets or extra neutral singlets, the decay mode $D^0 \to \mu\bar{e}$ can be generated (in a similar fashion as $K_L \to \mu\bar{e}$) only if there are non-degenerate neutrinos and nonzero neutrino mixings [51]. We display the relevant box-diagram in Fig. 15. The associated matrix element can be written as

$$\mathcal{M}_{D^0\to\mu\bar{e}} = \frac{G_F^2 M_W^2}{2\pi^2} f_D m_\mu B \; \bar{u}\Gamma_{\rm R} v \quad , \tag{93}$$

where B is given by [13]

$$\begin{aligned} B \;\equiv\; & \sum_{\alpha,k} U_{\alpha\mu}^* U_{\alpha e} V_{ck}^* V_{uk} x_\alpha x_k \Bigg[-\frac{1}{(1-x_\alpha)(1-x_k)} \\ & + \frac{1}{x_\alpha - x_k}\left(\frac{\ln x_k}{(1-x_k)^2} - \frac{\ln x_\alpha}{(1-x_\alpha)^2}\right)\Bigg] \quad . \end{aligned} \tag{94}$$

In the above, the greek and latin indices run respectively over the neutral leptons and negatively-charged quarks, $U_{\alpha\beta}$ and V_{jk} are respectively mixing-matrix elements for leptons and quarks, and $x_k \equiv m_k^2/M_W^2$. In the excellent approximation that $x_\alpha \simeq 0$ for $\alpha = \nu_e, \nu_\mu, \nu_\tau$ and $x_i = 0$ for $i = d$, the expression for B becomes [52]

$$\begin{aligned} B \;&=\; U_{\mu N} U_{\alpha N}^* \Bigg[V_{cs}^* V_{su} \left(\frac{x_s x_N}{1-x_N} - \ln x_s + \frac{\ln x_N}{(1-x_N)^2}\right) \\ &\qquad + V_{cb}^* V_{bu} \left(\frac{x_b x_N}{1-x_N} - \ln x_b + \frac{\ln x_N}{(1-x_N)^2}\right)\Bigg] \\ &\simeq\; 4.2 \times 10^{-5}\; U_{Ne}^* U_{N\mu} \end{aligned} \tag{95}$$

for a fourth generation neutral lepton mass of $m_N \simeq 50$ GeV. This result varies rather slowly as m_N increases to larger values up to and beyond M_W. The decay rate for $D^0 \to \mu\bar{e}$ is then given by

$$\Gamma_{D^0\to\mu\bar{e}} = \left[\frac{G_F^2 M_W^2 f_D m_\mu B}{4\pi^2}\right]^2 \frac{M_D}{4\pi} \left(U_{Ne} U_{N\mu}\right)^2 \quad . \tag{96}$$

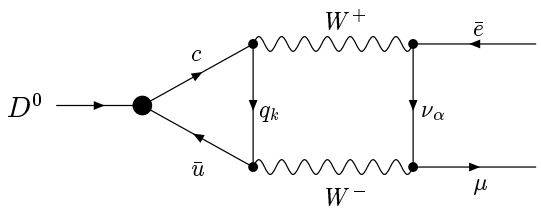

Figure 15: Box diagram mediating $D^0 \to \mu\bar{e}$.

The mixing $(U_{Ne}U_{N\mu})^2$ for $m_N > 50$ GeV is constrained by the limit on $\mathcal{B}r_{\mu\to e\gamma}$ to be [53,16] less than 5.6×10^{-8} and hence we infer

$$\Gamma_{D^0\to\mu\bar{e}} = \begin{cases} < 8.62 \times 10^{-27} \text{ GeV} & , \\ \leq 1.3 \times 10^{20} \text{ sec}^{-1} & . \end{cases} \tag{97}$$

The branching ratio for $D^0 \to \mu\bar{e}$ is thus bounded by

$$\mathcal{B}r_{D^0\to\mu^-e^+} \leq 5.2 \times 10^{-15} \qquad \text{or} \qquad \mathcal{B}r_{D^0\to\mu^-e^+ + \mu^+e^-} \leq 1.0 \times 10^{-14} \quad . \tag{98}$$

If the heavy neutral lepton N^0 is an $SU(2)$ singlet rather than a member of a doublet, the same result is obtained, even though the GIM suppression is absent [52,54]. Hence any observation of $D^0 \to \mu\bar{e}$ with $\mathcal{B}r_{D^0\to\mu\bar{e}} > 10^{-14}$ cannot be explained by mixing with a heavy neutrino.

3.2.4 Extra Dimensions

Attempts to address the hierarchy problem by exploiting the geometry of space-time have led to extra dimensional theories which have verifiable consequences at the TeV scale. These theories make use of the idea that our universe lies on a $(3+1)$-dimensional brane which is embedded in a higher D-dimensional space-time, $D \equiv (1+3+\delta)$, known as the bulk. The size and geometry of the bulk, as well as the field content which is allowed to propagate in the bulk, varies between different scenarios. Upon compactification of the additional dimensions, all bulk fields expand into a Kaluza-Klein (KK) tower of states on the $(3+1)$-brane, where the masses of the KK states correspond to the δ-dimensional kinetic motion of the bulk field. The direct observation or indirect effects of the KK states signals the existence of extra dimensions.

There are various potential contributions to rare decays within these scenarios:

(i) In the case of large, flat toroidal extra dimensions [55], gravity alone propagates in the bulk and the resultant bulk graviton KK tower states, G_n, couple with inverse Planck scale strength and have very fine mass splittings given by $1/R_c \sim 10^{-4}eV$ to a few MeV, where R_c is the common compactification radius of the additional dimensions. They may be radiated in rare decays such as $c \to u + G_n$ and subsequently appear as

missing energy. The bulk graviton KK states couple to the conserved stress-energy tensor, giving a contribution to this process of order m_c^2/M_D^2 where M_D is the fundamental scale of gravity in the higher dimensional space and is assumed to be of order a TeV in these models.

(ii) If the extra dimensions are of size TeV^{-1}, then the Standard Model gauge fields may propagate in the bulk and hence expand into KK towers [56]. The KK tower states of the γ, Z, W, and gluon may participate in rare transitions in a variety of ways. However, precision electroweak data constrain the mass of the first gauge KK excitation to be in excess of 4 TeV [57], and hence their contributions to rare decays are small [58].

(iii) If the Standard Model fermions are localized [59] at specific points within a TeV^{-1}-sized extra dimension, then they obtain narrow gaussian-like wave functions in the extra dimension with a width much smaller than the compactification radius. In this case, the fermion mass hierarchy may be explained and FCNC are suppressed by the small overlap of the wave functions for the different flavors.

(iv) The last possibility is the Randall-Sundrum model of localized gravity [60], based on a non-factorizable geometry in 5-dimensional Anti-de-Sitter space. In this case, the Standard Model gauge and matter fields, as well as gravity, are allowed to propagate in the warped extra dimension. The first bulk graviton KK excitation mass is of order a TeV and hence does not participate in rare decays. However, the first gauge and fermion KK excitations are lighter and may have interesting consequences in rare transitions [61]. In models of this type, it is possible [62] to generate tree-level FCNC which may produce observable effects in rare charm decays.

3.3 Strong Dynamics

The possibility that new strong interactions are responsible for electroweak symmetry breaking (EWSB) and/or fermion masses has important consequences for flavor physics. The SM with one Higgs doublet already requires the presence of new dynamics at a scale Λ in order to avoid triviality bounds. The physics above the cutoff scale gives rise to the scalar sector via bound states and is connected in some fashion to the the generation of flavor. For instance, technicolor theories require extended technicolor, whereas the generation of the (large) top quark mass may require a top-condensation mechanism. In general the generation of fermion mass textures leads, in one way or another, to FCNC. Here we examine some of the potential effects in rare charm decays and their relation to other phenomenological constraints.

3.3.1 Extended Technicolor

In standard technicolor theories both fermions and techni-fermions transform under the new gauge interaction of Extended Technicolor (ETC). The condensation of techni-fermions leading to EWSB leads to fermion mass terms of the form

$$m_q \simeq \frac{g_{\rm ETC}^2}{M_{\rm ETC}^2}\langle \bar{T}T\rangle_{\rm ETC} \quad . \tag{99}$$

The ETC interactions connect ordinary fermions with techni-fermions, as well as fermions and techni-fermions among themselves. The relevant sources of FCNC in technicolor models divide into two classes: those associated with the technicolor sector and those where the diagonal ETC gauge bosons acting on ordinary fermions give rise to FCNC through dimension-six operators.

The first case gives rise to operators mediated by ETC gauge bosons. These in turn have been shown [63] to give rise to FCNC involving the Z-boson,

$$\xi^2\frac{m_c}{8\pi v}\frac{e}{\sin 2\theta_W}U_{cu}^L Z^\mu\ (\bar{u}_L\gamma_\mu c_L) \quad \text{and} \quad \xi^2\frac{m_t}{8\pi v}\frac{e}{\sin 2\theta_W}U_{tu}^L U_{tc}^{L*} Z^\mu\ (\bar{u}_L\gamma_\mu c_L) \quad , \tag{100}$$

where U^L is the unitary matrix rotating left-handed up-type quark fields into their mass basis and ξ is a model-dependent quantity of $\mathcal{O}(1)$. The induced flavor-conserving Z coupling was first studied in Ref. [63] and flavor-changing effects in B decays have been examined in Refs. [64,65]. The flavor-changing vertices in Eq. (100) induce contributions to $c \to u\ell^+\ell^-$. These appear mostly as a shift in the Wilson coefficient $C_{10}(M_W)$,

$$\delta C_{10} \simeq U_{cu}^L\,\frac{m_c}{2v}\,\frac{\sin^2\theta_W}{\alpha} \simeq 0.02\ , \tag{101}$$

where we make the assumption $U_{cu}^L \simeq \lambda \simeq 0.22$ (*i.e.*, one power of the Cabibbo angle) and we take $m_c = 1.4$ GeV. Although this represents a very large enhancement with respect to the SM value of $C_{10}(M_W)$, it does not translate into a large deviation in the branching ratio. As mentioned previously, these are dominated by the mixing of the operator O_2 with O_9, leading to a very large value of $C_9^{\rm eff}$. The contribution in Eq. (101) represents only a few percent effect in the branching ratio with respect to the SM. On the other hand, the interaction in Eq. (100) can also mediate $D^0 \to \mu^+\mu^-$. The corresponding amplitude is

$$\mathcal{A}_{D^0\mu^+\mu^-} \simeq U_{cu}^L\,\frac{m_c}{2\pi v}\,\frac{G_F}{\sqrt{2}}\,\sin^2\theta_W f_D\, m_\mu\ , \tag{102}$$

which should be compared to Eq. (50). This results in the branching ratio $\mathcal{B}r_{D^0\to\mu^+\mu^-}^{\rm ETC} \simeq 0.6\times 10^{-10}$, which although still small, is not only several orders of magnitude larger than the SM short distance contribution but also more than two orders of magnitude larger than the long distance estimates.

Finally, the FCNC vertices of the Z boson in Eq. (100) also give large contributions to $c \to u\nu\bar{\nu}$. The enhancement is considerable and results in the branching ratio

$$\mathcal{B}r^{\rm ETC}_{D^+\to X_u\nu\bar{\nu}} \simeq \xi^4 \left(\frac{U^L_{cu}}{0.2}\right)^2 2\times 10^{-9} \ . \tag{103}$$

The second class of contributions from technicolor models comes from the diagonal ETC gauge bosons. These generate four-quark interactions which refer to a mass scale constrained by D^0-$\bar{D}^0$ mixing to be approximately $M > 100$ TeV [63], thus making such effects very small in rare charm decays.

3.3.2 Top-condensation Models

Top-condensation models postulate a new gauge interaction that is strong enough to break the top-quark chiral symmetry and give rise to the large top mass. The various realizations of this basic idea have one common feature: flavor violation. Since the new interaction must be non-universal, it mediates FCNC at tree level. This arises because the mass matrix generated between the top-condensate and the other flavor physics gives rise to the lighter fermion masses (*e.g.* ETC in topcolor-assisted technicolor [66]) and is not aligned with the weak basis. Diagonalization of this mass matrix will then leave FCNC vertices of the so-called 'topcolor interactions' since they couple preferentially to the third generation. The exchange of top-gluons and topcolor gauge bosons will generate four-fermion couplings of the form

$$\begin{aligned}
&\frac{4\pi\alpha_s \cot\theta^2}{M^2}\, U^*_{tc}U_{tu}\,(\bar{u}\gamma_\mu T^a t)(\bar{t}\gamma^\mu T^a c)\\
&\frac{4\pi\alpha_s \tan\theta^2}{M^2}\, U_{cu}\,(\bar{u}\gamma_\mu T^a c)(\bar{c}\gamma^\mu T^a c)\\
&\frac{4\pi\alpha_s}{M^2}\, U_{cu}\,(\bar{u}\gamma_\mu T^a c)(\bar{\xi}\gamma^\mu T^a \xi) \ ,
\end{aligned} \tag{104}$$

where $\xi^T \equiv (t\ b)$, $U_{ij} = U^L_{ij} + U^R_{ij}$ and M is the mass of the exchanged color-octet gauge boson. The first term comes from rotating two top-quark fields via the strongly coupled topgluon, with the strong interaction being reflected in the factor $\cot^2\theta \simeq 22$. The second term corresponds to a topgluon which is weakly coupled to the first and second generations. In the third term, which gives the largest contribution, the topgluon couples strongly to the third generation quark current but weakly to the $(\bar{u}c)$ current, giving rise to a gluon-like coupling. The one-loop insertion of the first and/or third terms in Eq. (104) would result in contributions to the operators $\mathcal{O}_9$ and $\mathcal{O}_{10}$. However, a term analogous to the *second* term in Eq. (104) but with the $\bar{c}_L$ quark rotated to a $\bar{u}_L$ would contribute to D^0-$\bar{D}^0$ mixing. The current experimental bound on Δm_D taken from Eq. (68) implies

that

$$\frac{M}{Re[U_{cu}]} > 140 \text{ TeV} . \tag{105}$$

In standard Topcolor Assisted Technicolor models, this constraint is not binding on the top-gluon mass since the up-sector rotation matrices are taken to be nearly diagonal [67]. However, once it is satisfied, the bound of Eq. (105) implies that all effects in rare charm decays are negligible. Similarly, this also applies to the topcolor Z' arising from the strongly coupled $U(1)_Y$.

4 Conclusions

We have extensively evaluated the potential of rare charm decays to probe physics beyond the SM. In Section 2 we computed the SM rates for a variety of decay modes; incorporating the first evaluation of the QCD corrections to the short distance contributions, as well as a comprehensive study of long range effects. This extends our earlier work in Ref. [5], where we concentrated solely on radiative decays. We have shown that although, just as in the radiative modes, it is still true that long distance contributions dominate the rates, there *are* decay channels where it is possible to access the short distance physics. This is particularly true for the case of $D \to X_u \ell^+ \ell^-$ decay modes such as $D \to \pi \ell^+ \ell^-$ and $D \to \rho \ell^+ \ell^-$, away from the resonance contributions in the low dilepton mass region. This is illustrated in Figs. 1 and 2, where we see that for low dilepton invariant mass the sum of long and short distance effects leaves a large window where physics beyond the SM can be observed. Although the uncertainties in our calculation of the long distance contributions to this mode are still sizable (roughly of $\mathcal{O}(1)$) it is clear that at low dilepton masses new physics effects that are an order of magnitude or more larger than the short distance SM signal can be detected. This is not the case in the resonance region where the ϕ, ω and ρ contributions take the rates to values just below current experimental bounds, in a situation analogous with radiative decays such as $D \to \rho\gamma$. We compile our predictions for the SM rates in Table 6.

In Section 3 we explored the potential of these decays to constrain new physics. In the case of the MSSM, we examined the sensitivity of rare charm decays to non-universal soft breaking in the squark mass matrices. We found that large effects are possible in $D \to \pi \ell^+ \ell^-$ and particularly in $D \to \rho \ell^+ \ell^-$, as can be seen from Figures 10 and 11. The effect in the vector mode is amplified by the heightened sensitivity of this decay channel to the photonic penguin, which carries a large enhancement since the gluino helicity flip replaces the usual charm quark mass insertion. This effect, unfortunately, is obscured in radiative decays such as $D \to \rho\gamma$ due to the overwhelming long range effects. It can therefore, only be observed by examination of the full dilepton mass spectrum in $D \to X \ell^+ \ell^-$. We conclude that an important fraction of parameter space in the MSSM

with non-universal soft breaking can be explored if sensitivities of the order of 10^{-6} to 10^{-7} in the kinematic region of interest are reached.

We also considered the effects of R-parity violating couplings in supersymmetry. We found that the current upper limit on the decay $D \to \pi\mu^+\mu^-$ yields the best constraint on the product $\tilde{\lambda}'_{22k}\,\tilde{\lambda}'_{21k}$ (see Eq. (78)). Thus rare charm decays already constrain R-parity violating effects! Our results are summarized in Table 5 for the predictions with R-parity violation effects, assuming the couplings saturate their current bounds. We have also shown that the forward-backward asymmetry for leptons A_{FB} in $D^0 \to \rho^0\ell^+\ell^-$ is quite sensitive to these effects (*cf.* Figure 14). More generally, A_{FB} is negligibly small in the SM due to the fact that the vector coupling of leptons is enormously enhanced with respect to the axial-vector coupling by the presence of vector mesons. Thus, any observation of A_{FB} would point to the presence of new physics.

We also considered the effects of other non-supersymmetric extensions of the SM including multi-Higgs models, horizontal gauge models, a fourth generation, extra dimensions, as well as models with strong dynamics such as extended technicolor and topcolor. These scenarios give sizeable enhancements in some of the modes.

We conclude that these rare charm decay modes are most sensitive to the effects of non-universal supersymmetry breaking as well as to R-parity violating couplings. It is then important to push for increased sensitivity of the experiments, preferably to below 10^{-6} in order to highly constrain these effects. This is in stark contrast with the situation in the radiative modes, where sensitivity below $10^{-5} - 10^{-6}$ may not illuminate short distance physics. The dilepton modes should be pursued by all facilities to highest possible sensitivity.

Acknowledgments The authors acknowledge among others Jeff Appel, Dan Kaplan and Boris Kayser for their encouragement and motivation, Xerxes Tata for helpful discussions, and Jeff Appel and Paul Singer for a careful reading of the paper. The work of G.B was supported by the Director, Office of Science, Office of High Energy and Nuclear Physics of the U.S. Department of Energy under Contract DE-AC0376SF00098. The work of E.G. was supported in part by the National Science Foundation under Grant PHY-9801875. The research of J.H. is supported by the Department of Energy, Contract DE-AC03-76SF00515. S.P. was supported in part by the US DOE under grant DE-FG 03-94ER40833.

Decay Mode	Experimental Limit	$\mathcal{B}r_{S.D.}$	$\mathcal{B}r_{L.D.}$
$D^+ \to X_u^+ e^+ e^-$		2×10^{-8}	
$D^+ \to \pi^+ e^+ e^-$	$< 4.5 \times 10^{-5}$		2×10^{-6}
$D^+ \to \pi^+ \mu^+ \mu^-$	$< 1.5 \times 10^{-5}$		1.9×10^{-6}
$D^+ \to \rho^+ e^+ e^-$	$< 1.0 \times 10^{-4}$		4.5×10^{-6}
$D^0 \to X_u^0 e^+ e^-$		0.8×10^{-8}	
$D^0 \to \pi^0 e^+ e^-$	$< 6.6 \times 10^{-5}$		0.8×10^{-6}
$D^0 \to \rho^0 e^+ e^-$	$< 5.8 \times 10^{-4}$		1.8×10^{-6}
$D^0 \to \rho^0 \mu^+ \mu^-$	$< 2.3 \times 10^{-4}$		1.8×10^{-6}
$D^+ \to X_u^+ \nu \bar{\nu}$		1.2×10^{-15}	
$D^+ \to \pi^+ \nu \bar{\nu}$			5×10^{-16}
$D^0 \to \bar{K}^0 \nu \bar{\nu}$			2.4×10^{-16}
$D_s \to \pi^+ \nu \bar{\nu}$			8×10^{-15}
$D^0 \to \gamma\gamma$		3×10^{-11}	few $\times 10^{-8}$
$D^0 \to \mu^+ \mu^-$	$< 3.3 \times 10^{-6}$	10^{-18}	few $\times 10^{-13}$
$D^0 \to e^+ e^-$	$< 1.3 \times 10^{-5}$	$(2.3 - 4.7) \times 10^{-24}$	
$D^0 \to \mu^\pm e^\mp$	$< 8.1 \times 10^{-6}$	0	0
$D^+ \to \pi^+ \mu^\pm e^\mp$	$< 3.4 \times 10^{-5}$	0	0
$D^0 \to \rho^0 \mu^\pm e^\mp$	$< 4.9 \times 10^{-5}$	0	0

Table 6: Standard Model predictions for the branching fractions due to short and long distance contributions for various rare D meson decays. Also shown are the current experimental limits [16],[35],[41].

References

[1] D. Abbaneo *et al.*, Combined LEP Electroweak and SLD Electroweak and Heavy Flavor Working Groups, LEPEWWG/2001-01.

[2] A. Datta and D. Kumbhakhar, Zeit. Phys. **C27**, 515 (1985); J. Donoghue, E. Golowich, B. Holstein and J. Trampetic, Phys. Rev. **D33**, 179 (1986); L. Wolfenstein, Phys. Lett. **B164**, 170 (1985); H. Georgi, Phys. Lett. **B297**, 353 (1992); T. Ohl *et al.*, Nucl. Phys. **B403**, 605 (1993); A.A. Petrov, Phys. Rev. **D56**, 1685 (1997).

[3] E. Golowich and A.A. Petrov, Phys. Lett. **B427**, 172 (1998).

[4] A. F. Falk, Y. Grossman, Z. Ligeti and A. A. Petrov, "$SU(3)$ *breaking and* D^0-$\bar{D}^0$ *mixing*", Phys. Rev. D (to appear); hep-ph/0110317.

[5] G. Burdman, E. Golowich, J. Hewett and S. Pakvasa, Phys. Rev. **D52**, 6383 (1995).

[6] C. Greub *et al.*, Phys. Lett. **B382**, 415 (1996).

[7] B. Bajc, S. Fajfer and R. J. Oakes, Phys. Rev. **D54**, 5883 (1996); S. Fajfer, S. Prelovsek and P. Singer, Eur. Phys. J. **C6**, 471 (1999).

[8] G. Brandenburg *et al.*, the CLEO collaboration, Phys. Rev. Lett. **87**, 071802 (2001).

[9] H. N. Nelson, *"Compilation of* $D^0 \to \bar{D}^0$ *mixing predictions"*, in Proc. of the 19th Intl. Symp. on Photon and Lepton Interactions at High Energy LP99, ed. J.A. Jaros and M.E. Peskin, hep-ex/9908021; J.L. Hewett, T. Takeuchi, and S. Thomas in *Electroweak Symmetry Breaking and New Physics at the TeV Scale*, ed. T. Barklow *et al.*, (World Scientific, Singapore 1996), hep-ph/9603391.

[10] S. Fajfer, S. Prelovsek and P. Singer, Phys. Rev. **D58**, 094038 (1998).

[11] S. Fajfer, S. Prelovsek and P. Singer, Phys. Rev. **D64**, 114009 (2001).

[12] F. J. Gilman and M. B. Wise, Phys. Rev. **D20**, 2392 (1979).

[13] T. Inami and C.S. Lim, Prog. Theor. Phys. **65**, 1772 (1981).

[14] G. Buchalla, A. J. Buras and M. E. Lautenbacher, Rev. Mod. Phys. **68**, 1125 (1996).

[15] P. Singer and D.-X. Zhang, Phys. Rev. **D55**, R1127 (1997).

[16] D.E. Groom *et al.*, Particle Data Group, Eur. Phys. J. **C15**, 1 (2000).

[17] C. S. Lim, T. Morozumi and A. I. Sanda, Phys. Lett. **B218**, 343 (1989); N.G. Deshpande, J. Trampetic, and K. Panrose, Phys. Rev. **D39**, 1461 (1989).

[18] N. Isgur and M. B. Wise, Phys. Rev. **D42**, 2388 (1990).

[19] G. Burdman and J. F. Donoghue, Phys. Lett. **B280**, 287 (1992); M. B. Wise, Phys. Rev. **D45**, 2188 (1992).

[20] A. Anastassov *et al.*, the CLEO Collaboration, Phys. Rev. **D65**, 032003 (2002).

[21] K. Kodama *et al.*, the Fermilab E653 Collaboration, Phys. Lett. **B274**, 246 (1992); P. L. Frabetti *et al.*, the Fermilab E687 Collaboration, Phys. Lett. **B307**, 262 (1993).

[22] E. Golowich and S. Pakvasa, Phys. Rev. **D51**, 1215 (1995).

[23] J. M. Soares, Phys. Rev. **D53**, 241 (1996).

[24] M. Beneke, G. Buchalla, M. Neubert and C. T. Sachrajda, Phys. Rev. Lett. **83**, 1914 (1999); and Nucl. Phys. **B591**, 313 (2000).

[25] M. Acciarri *et al.*, the L3 Collaboration, Phys. Lett. **B396**, 327 (1997).

[26] C-H. V. Chang, G-L. Lin and Y-P. Yao, Phys. Lett. **B415**, 395 (1997); L. Reina, G. Ricciardi and A. Soni, Phys. Rev. **D56**, 5805 (1997).

[27] D. Choudhury and J. Ellis, Phys. Lett. **B433**, 102 (1998).

[28] S. Fajfer, P. Singer and J. Zupan, Phys. Rev. **D64**, 074008 (2001).

[29] L.J. Hall, V.A. Kostelecky, and S. Raby, Nucl. Phys. **B267**, 415 (1986).

[30] For a comprehensive study of FCNC effects in supersymmetry see, S. Bertolini, F. Borzumati, A. Masiero, and G. Ridolfi, Nucl. Phys. **B193**, 591 (1991); F. Gabbiani, E. Gabrielli, A. Masiero and L. Silvestrini, Nucl. Phys. **B477**, 321 (1996); J.L. Hewett and J.D. Wells, Phys. Rev. **D55**, 5549 (1997); P. Cho, M. Misiak, and D. Wyler, Phys. Rev. **D54**, 3329 (1996). For a review see M. Misiak, S. Pokorski and J. Rosiek, in "*Heavy Flavors II*", eds. A.J. Buras and M. Lindner, Adv. Ser. Direct. High Energy Phys. **15**, 795 (1998).

[31] See, for example, J. Ellis and D.V. Nanopoulos, Phys. Lett. **110B**, 44 (1982).

[32] E. Lunghi, A. Masiero, I. Scimemi and L. Silvestrini, Nucl. Phys. **B568**, 120 (2000).

[33] S. Prelovsek and D. Wyler, Phys. Lett. **B500**, 304 (2001).

[34] J. A. Casas and S. Dimopoulos, Phys. Lett. **B387**, 107 (1996).

[35] E. Aitala *et al.*, Phys. Lett. **B462**, 401 (1999).

[36] See, for example, L.E. Ibanez and G.G. Ross, Nucl. Phys. **B386**, 3 (1992).

[37] For a recent review, see, B. C. Allanach, A. Dedes and H. K. Dreiner, Phys. Rev. **D60**, 075014 (1999).

[38] K. Agashe and M. Graesser, Phys. Rev. **D54**, 4445 (1996).

[39] S. Adler *et al.*, E787 collaboration, Phys. Rev. Lett. **84**, 3768 (2000), and hep-ex/0111091.

[40] G. Bhattacharyya and D. Choudhury, Mod. Phys. Lett. **A10**, 1699 (1995).

[41] E. Aitala *et al.*, Phys. Rev. Lett. **86**, 3969 (2001).

[42] A. Ali, T. Mannel and T. Morozumi, Phys. Lett. **B273**, 505 (1991);

[43] G. Burdman, Phys. Rev. **D52**, 6400 (1995); Phys. Rev. **D57**, 4254 (1998).

[44] C. Greub, A. Ioannissian, and D. Wyler, Phys. Lett. **B346**, 149 (1995); D. Liu, Phys Rev. **D52**, 5056 (1995); A. Ali *et al.*, Phys. Rev. **D61**, 074024 (2000).

[45] See, for example, W. Molzon in *Beyond the Desert 1999: Accelerator, Non-Accelerator, and Space Approaches into the Next Millennium*, ed. H.V. Klapdor-Kleingrothaus and I.V. Krivosheina (Inst. of Physics, Bristol 2000).

[46] S. Pakvasa and H. Sugawara, Phys. Lett. **B73**, 61 (1978).

[47] L. Hall and S. Weinberg, Phys. Rev. **D48**, 979 (1993); A. Joshipura, Phys. Rev. **D39**, 878 (1989); K.S. Babu and S. Nandi, hep-ph/9907293; D. Atwood, L. Reina and A. Soni, Phys. Rev. **D55**, 3156 (1997); J. Bordes *et al.*, Phys. Rev. **D60**, 013005 (1999); T. Brown *et al.*, Phys. Lett. **B141**, 95 (1984); T.P. Cheng and M. Sher, Phys. Rev. **D35**, 3484 (1987).

[48] G. Volkov, V. A. Monich and B. Struminski, Yad. Fiz. **34**, 435 (1981); S. Weinberg, UTTG-05-91, Proceedings, *High Energy Physics and Cosmology*, Islamabad, M. A. B. Bég Memorial Volume; H. N. Long and V. T. Van, hep-ph/9903902. A good list of references to many earlier works on horizontal gauge symmetric models can be found in *e.g.*, D. S. Shaw and R. R. Volkas, Phys. Rev. **D47**, 241 (1993).

[49] J.L. Hewett and T.G. Rizzo, Phys. Rept. **183**, 193 (1989).

[50] K.S. Babu, X-G. He, X-Q. Li and S. Pakvasa, Phys. Lett. **B205**, 540 (1988).

[51] B.W. Lee, S. Pakvasa, R. Shrock and H. Sugawara, Phys. Rev. Lett. **38**, 937 (1977).

[52] P. Langacker, S. Uma Sankar and K. Schlicher, Phys. Rev. **D38**, 2841 (1988); A. Barroso *et al.*, Phys. Lett. **B134**, 123 (1984).

[53] A. Acker and S. Pakvasa, Mod. Phys. Lett. **A7**, 1219 (1992) .

[54] Z. Gagyi-Palffy, A. Pilaftsis and K. Schilcher, Phys. Lett. **B343**, 275 (1995).

[55] N. Arkani-Hamed, S. Dimopoulos, and G. Dvali, Phys. Lett. **B429**, 263 (1998), and Phys. Rev. **D59**, 086004 (1999); I. Antoniadis, N. Arkani-Hamed, S. Dimopoulos, and G. Dvali, Phys. Lett. **B436**, 257 (1998).

[56] I. Antoniadis, Phys. Lett. **B246**, 377 (1990); J. Lykken, Phys. Rev. **D54**, 3693 (1996); E. Witten, Nucl. Phys. **B471**, 135 (1996); P. Horava and E. Witten, Nucl. Phys. **B460**, 506 (1996), *ibid.*, **B475**, 94 (1996).

[57] T.G. Rizzo and J.D. Wells, Phys. Rev. **D61**, 016007 (2000); P. Nath and M. Yamaguchi, Phys. Rev. **D60**, 116006 (1999); M. Masip and A. Pomarol, Phys. Rev. **D60**, 096005 (1999); W.J. Marciano, Phys. Rev. **D60**, 093006 (1999).

[58] See, for example, K. Agashe, N.G. Deshpande, G.H. Wu, Phys. Lett. **B514**, 309 (2001).

[59] N. Arkani-Hamed and M. Schmaltz, Phys. Rev. **D61**, 033005 (2000).

[60] L. Randall and R. Sundrum, Phys. Rev. Lett. **83**, 3370 1999 , and *ibid.*, 4690, (1999).

[61] H. Davoudiasl, J.L. Hewett, and T.G. Rizzo, Phys. Rev. **63**, 075004 (2001); S. Chang *et al.*, Phys. Rev. **D62**, 084025 (2000); T. Ghergetta and A. Pomarol, Nucl. Phys. **B586**, 141 (2000).

[62] J.L. Hewett, F.J. Petriello, and T.G. Rizzo, SLAC-PUB-9146.

[63] R. S. Chivukula, S. B. Selipsky and E. H. Simmons, Phys. Rev. Lett. **69**, 575 (1992).

[64] L. J. Randall and R. Sundrum, Phys. Lett. **B312**, 148 (1993).

[65] B. Grinstein, Y. Nir and J. M. Soares, Phys. Rev. **D48**, 3960 (1993).

[66] C. T. Hill, Phys. Lett. **B266**, 419 (1991); C. T. Hill, Phys. Lett. **B345**, 483 (1995); K. Lane and E. Eichten, Phys. Lett. **B352**, 382 (1995).

[67] G. Burdman, K. D. Lane and T. Rador, Phys. Lett. **B514**, 41 (2001).

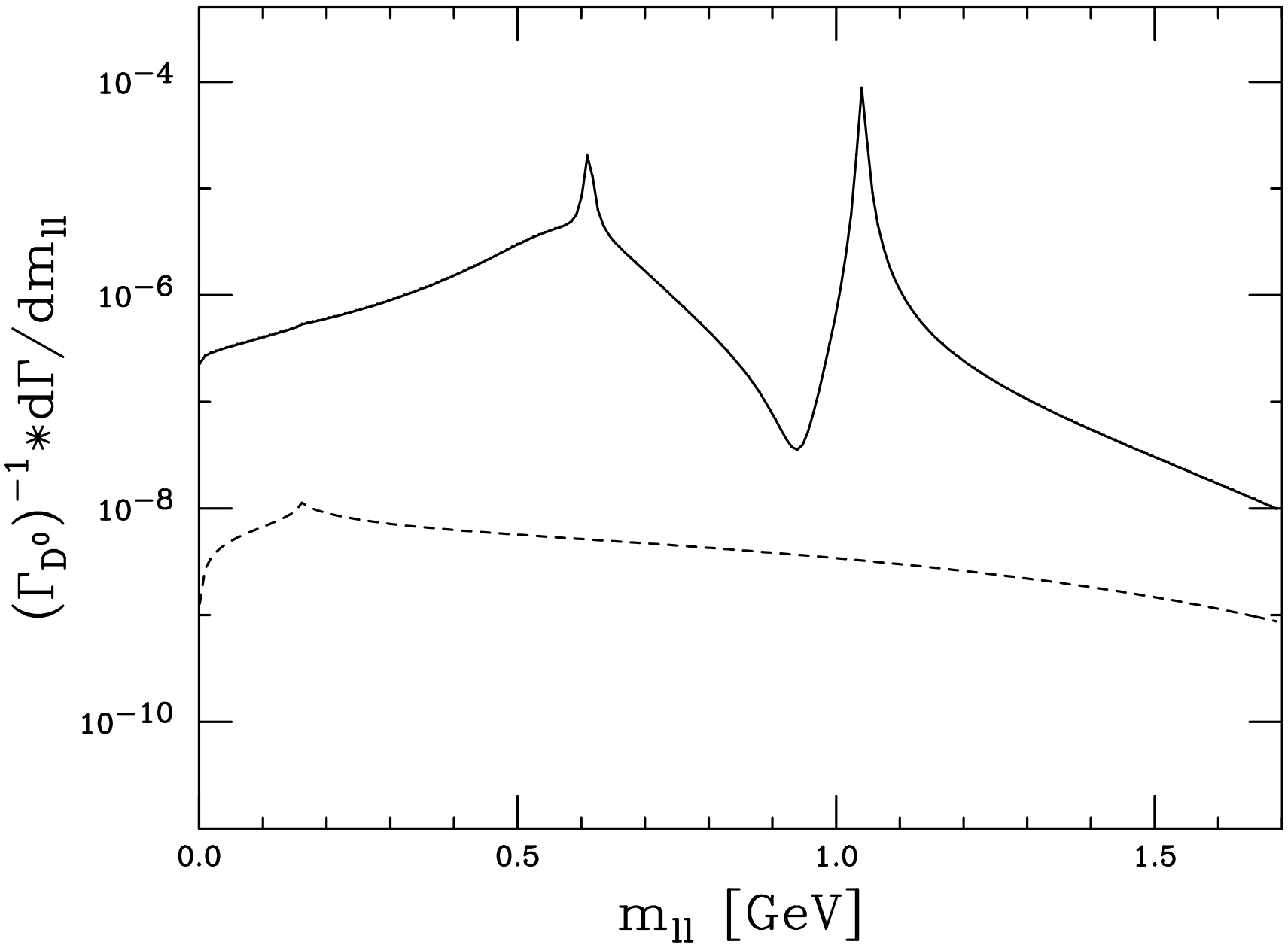
10^{-4}
10^{-6}
10^{-8}
10^{-10}
$(\Gamma_{D^0})^{-1} * d\Gamma/dm_{ll}$
0.0
0.5
1.0
1.5
m_{ll} [GeV]